CHARLES UNIVERSITY IN PRAGUE

FACULTY OF PHARMACY IN HRADEC KRÁLOVÉ

Department of pharmaceutical technology

UNIVERSITY OF VALENCIA

FACULTY OF PHARMACY

Department of pharmacy and pharmaceutical technology

NORTRIPTYLINE HYDROCHLORIDE TRANSDERMAL DELIVERY FROM HMPC PATCH: EFFECT OF CONCENTRATION

UVOLŇOVÁNÍ HYDROCHLORIDU NORTRIPTYLINU Z TRANSDERMÁLNÍHO HPMC FILMU: VLIV KONCENTRACE

Diploma thesis

Diplomová práce

Ivana Heřmanová

May, 2008

CONTENTS

DECLARATION

Hereby I affirm in lieu of an oath, that I made the present thesis autonomously and without other than the indicated auxiliary means. The data used indirectly or from other sources, and concepts are characterized with list of sources.

Prohlašuji, že tato práce je mým původním autorským dílem, které jsem vypracovala samostatně. Veškerá literatura a další zdroje, z nichž jsem při zpracování čerpala, jsou uvedeny v seznamu použité literatury a v práci řádně citovány.

_____

Ivana Heřmanová

ABSTRACT

The objective of this study is to optimize a nortryptiline hydrochloride patch previously designed (1) with the intended aim to develop controlled drug release system as a smoking cessation aid.

Patches of 5%, 7.5% and 10% NTH concentrations were assayed for physical experiments. Measured thickness of the patches remains constant regardless of the NTH concentration. Obtained values are 31.88±5.0 μm, 32.33±5.1 μm and 32.00±3.8 μm for 5%, 7.5% and 10% patch respectively. The variability is lower than 20 % in every case. Release and penetration studies were performed using Franz type of diffusion cells. The maximum cumulative amount released from assayed patches at 7 hours (last sampling point) varies as a function of the NTH concentration. Two kinetic models, power law and first order kinetics, are useful in order to predict the maximum amount to be released and the rate at which the process will be developed. Taking first order results into account, the maximum amount to be released (Qinf) is 7.185±0.30[mg/cm^2]; 12.359±0.69[mg/cm^2]; and 29.333 ±1.97 [mg/cm^2] for 5%; 7.5% and 10%patch respectively. Considering the power law fitting, the main conclusion is that the release mechanism is basically fickian diffusion as the exponent is about 0.5. Estimated permeation parameters are Kp=0.019·10^{-3}±0.00 [cm/h]; t0=51.273±2.42[h] for 5% patch, Kp=0.004·10^{-3}±0.00 [mg/cm]; t0=28.099±1.97[h] for 7.5% patch and Kp=0.005·10^{-3}±0,00[mg/cm]; t0=26.312±1.98[h] for 10%patch. The lag time is decreases as the patch concentration is increased. Calculated flux is 0.834·10^{-6} and 1.291·10^{-6} [mg^{2}cm/g] for 7.5% and 10%patch respectively. Considering both parameters, flux and lug time, 10% patch is better dosage form than the other two.

ABSTRACT

Předmětem této studie je optimalizace dříve navrhnutého filmu obsahujícího hydrochlorid nortriptylinu (HNT), s cílem vyvinout transdermální terapeutický systém s kontrolovaným uvolňováním, který by byl použit jako pomoc při odvykání kouření.

Filmy s 5%, 7.5% respektive 10% obsahem HNT byly podrobeny fyzikálním zkouškám. Změřená tloušťka filmu byla konstantní, bez ohledu na koncentraci HNT. Obdržené hodnoty jsou 31.88±5.0 μm, 32.33±5.1 μm a 32.00±3.8 μm pro 5%, 7.5% respektive 10% film. Ve všech případech je variabilita nižší než 20%. Studie penetrace a uvolňování HNT byly provedeny s použitím difusních cel Franzova typu. Maximální celkové množství uvolněné ze zkoušeného filmu v čase 7 hodin, (čas posledního odběru vzorku), se měnilo jako funkce koncentrace HNT obsaženého ve filmu. Dva kinetické modely, power law a kinetiku prvního řádu, lze použít na výpočet maximálního předpokládaného množství, které se uvolní (Qinf). Pokud bereme v úvahu výsledky kinetiky prvního řádu, (Qinf) je 7.185±0.30[mg/cm^2]; 12.359±0.69[mg/cm^2]; a 29.333 ±1.97 [mg/cm^2] pro 5%; 7.5% respektive 10%film. Vzhledem k tomu, že exponent power law nabývá hodnot okolo 0.5, lze dojít k závěru, že k uvolňování látky dochází prostou difusí. Parametry vyhodnocené pro permeaci jsou Kp=0.019·10^{-3}±0.00 [cm/h]; t0=51.273±2.42[h] pro 5% film, Kp=0.004·10^{-3}±0.00 [mg/cm]; t0=28.099±1.97[h] pro 7.5% film a Kp=0.005·10^{-3}±0,00[mg/cm]; t0=26.312±1.98[h] pro 10%film. Lag time se snižuje se zvyšující se koncentrací filmu. Vypočítaný flux (J) nabývá hodnot 0.834·10^{-6} 1.291·10^{-6} [mg^{2}cm/g] pro 7.5% respektive 10% film. Pokud vezmeme v úvahu oba parametry, flux i lag time, 10%film je výhodnější dávkovací forma než film s obsahem HNT 5% respektive 7.5%.

1. INTRODUCTION

The World Health Organization (WHO) reports that tobacco is the leading preventable cause of death in the world. In 2005, tobacco caused 5.4million deaths. At the current rate, the death toll is projected to reach more than 8 million annually by 2030 and a total of up to one billion deaths in the 21st century. The smoking of cigarettes is one of the main risk factor for a number of chronic diseases, including cancer, lung disease, and cardiovascular diseases. Second-hand tobacco smoke is also dangerous to health. It causes cancer, heart diseases and many other serious diseases in adults. Almost half of the world's children breathe air polluted by tobacco smoke, which worsens their asthma conditions and causes dangerous diseases. At least 200000 workers die every year due to exposure to second-hand smoke at work. In Europe millions of smokers want to stop smoking and many have tried to do so but have difficulty succeeding because tobacco use is such a powerful addiction.(2)

The major inducer of tobacco dependence is nicotine, a tertiary amine with sympathomimetic activity. Nicotine was declared an addictive drug similar to heroin or cocaine. Nicotine itself is probably not responsible for most of the negative health consequences of smoking. Instead, persons who stop using nicotine-containing tobacco products experience an unpleasant withdrawal syndrome that may include such symptoms as depressed mood, disrupted sleep, irritability, frustration, anger, anxiety, difficulty concentrating, restlessness, decreased heart rate, and increased appetite or weight gain.(3) The extremely unpleasant nature of withdrawal from tobacco helps explain why many people who make an effort to stop smoking start up again.

Tobacco dependence pharmacological treatment is at the moment based on two strategies: nicotine replacement therapy and non-nicotine therapy. Nicotine replacement products (gum, patch, nasal spray and inhaler) delivers nicotine in a way that allows an individual to reduce nicotine withdrawal symptoms. The other smoking cessation pharmacotherapy uses sustained-release bupropion,

an aminoketone antidepressant, that is hypothesized to aid smoking cessation by inhibiting dopamine reuptake in mesolimbic dopamine system.(4)

There is a growing evidence, that nortriptyline hydrochloride, a tricyclic antidepressant, aids long-term smoking cessation. The evidence suggests that the mode of action is independent of its antidepressants effect and it is of similar efficacy to nicotine replacement.(5) There is also study showing that NTH permeates through the skin by passive diffusion.(1) Development of a transdermal drug delivery system (TDS) could be real alternative to oral administration offering a possible approach to overcome some of the drawbacks of systemic NTH oral therapy. Among the advantages of transdermal drug delivery system are also improving of patient compliance, assurance of essentially constant drug input and overcoming the gastrointestinal tract and the liver sites of metabolism that are responsible of the low oral bioavailability.

The object of this study was to optimize a nortryptiline patch previously designed.(1) It is a (hydroxypropyl) methyl cellulose matrix prepared with mixture of water, ethanol and propylene glycol as solvent system and oleic acid and polysorbate as penetration enhancer. The effect of NTH concentration on the release and penetration characteristics is established.

2. THEORY

2.1. STRUCTURE AND FUNCTION OF HUMAN SKIN

The skin is a complex organ covering the whole surface of the body. It is the largest organ of the body with a size of about 1.8 m^2 and weights approximately 4 kg. The thickness of the skin ranges from 1 mm to 4 mm. It varies from place to place over the body. (6)

Human skin provides an excellent barrier between the external environment and the body. It is a self repairing composite membrane which protects against physical, chemical, microbial, and radiological attack and performs a homeostatic role by controlling moisture and heat loss from the body. It also serves as a food reserve and sensory organ transmitting external environmental information.

Human skin may be subdivided into three mutually dependent layers (Figure 1) including from top to bottom: a) the epidermis (and its associated appendages, pilosebaceous follicles and sweat glands); b) the dermis, separated from the epidermis by the dermal-epidermal junction, and c) the hypodermis.

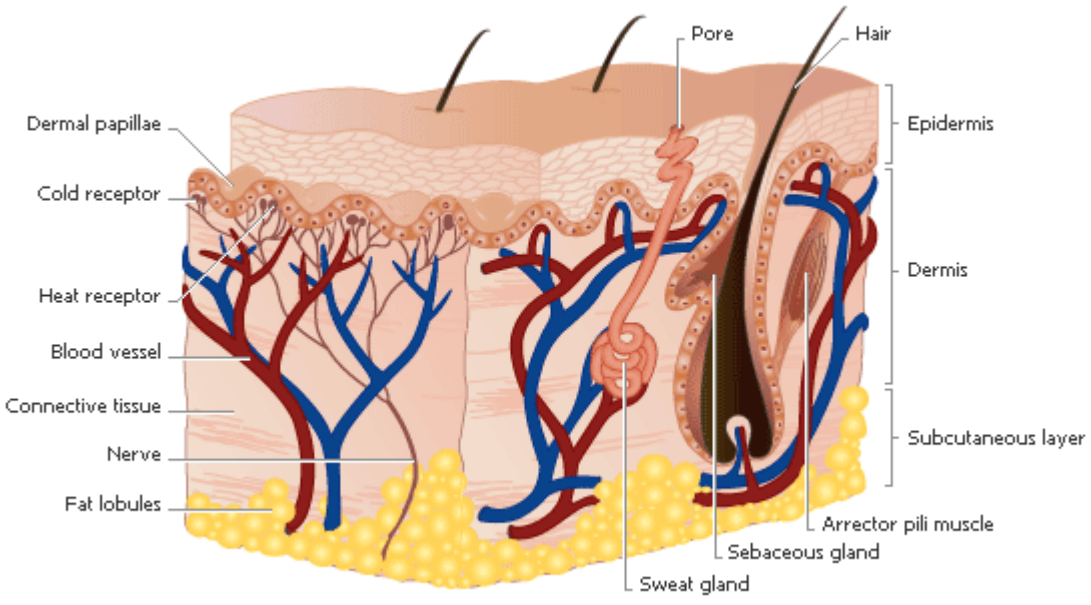

Figure 1: Anatomy of the skin (http://www.rush.edu/rumc/images/ei0390.gif)

2.1.1.The epidermis

The epidermis (Figure 2) is the outermost layer of the skin with thickness 0.06 to 0.1 mm. The cells of epidermis are arranged in continuous layers, comprising (from bottom to top):

- the stratum basale (basal layer or stratum germinativum)
- the stratum spinosum (spinous layer, princkle cell layer)
- the stratum granulosum (granular layer)
- the stratum corneum (horny layer)

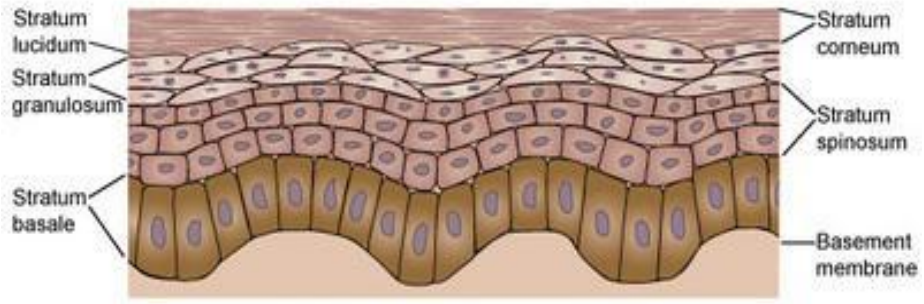

Figure 2: The epidermis anatomy (http://z.about.com/d/dermatology/1/.jpg)

The basal layer is a single layer of cubical or columnar, metabolically active cells. The principal cells of the basal layer are keratinocytes. The keratinocytes undergo cell division (via mitosis). On average, dividing basal cells replicate once every 200hours to 400 hours. After the replication, one daughter cell remains in the basal layer whilst the other migrates upwards through the epidermis towards the skin surface. The keratinocytes of the stratum basale are attached to the basement membrane by hemidesmosomes.

Five to ten per cent of epidermal cells are non-keratinocytes, including mainly Langerhans cells and melanocytes.

Langerhans cells function as antigen-presenting cells in the skin's immunological responses. Under the influence of melanocyte-stimulating hormone (MHS), melanocytes synthesize the pigment that gives the races of

humans their unique skin colorations. Melanocytes are also set into action by ultraviolet radiation, leading to suntanning.

The Merkel cell, other specialised cell type found within the basal layer, are associated with nerve endings. They have a role in cutaneous sensation.

The cells of *the spinous layer* exhibit sharp surface protuberances and begin to synthesise keratines that aggregate to form tonofilaments.

The major changes in cellular architecture occur in *the granular layer.* The cells of this layer continue to flatten and become much wider than underlying cells.

The outermost layer of the skin, *the stratum corneum* (Figure 3), is the main element of the skin's permeation barrier. (7) It is the end product of epidermal differentiation and consists of 15 to 25 cell layers over most of the body surface, though it is the much thicker over the palms and soles.(8) Each cell (corneocyte) is approximately 0.5 μm in thickness and 30 to 40 μm in width, the largest cell in epidermis. It contains no organelles but is filled with protein, 80 % if which is high molecular keratin (>60 000Daltons). The intercellular space is filled with lipids organized as bilayers. The stratum corneum has a very law water content, though it can take up to five times its weight in water when placed in a aqueous environment.(9)

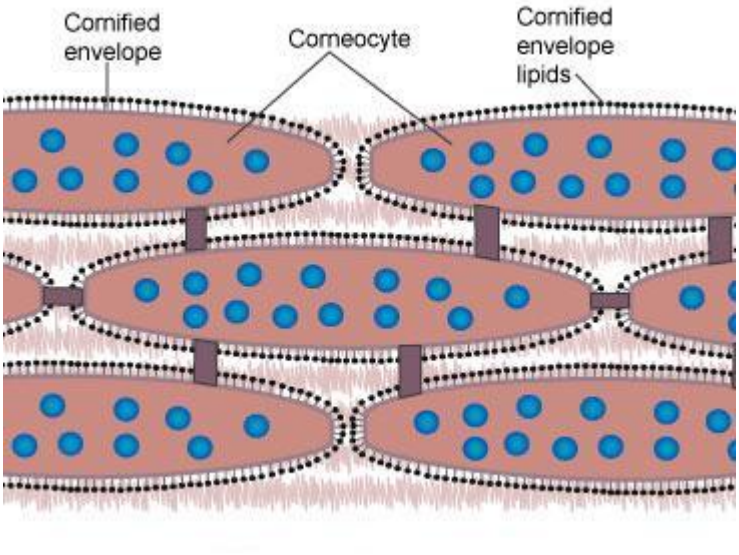

Figure 3: Stratum corneum anatomy (http://z.about.com/d/dermatology/1/.jpg)

The „brick and mortar model“(Figure 4) can be used to describe the structure of the horny layer. Corneocytes are the „bricks“ embedded in an intercellular lipid matrix of mainly fatty acids, ceramides, cholesterol and cholesterol sulfate.(10) Thus, the corneocytes are with a compound cell envelope, consisting of a highly insoluble, cross-linked protein inner surface and a hydroxyceramide monolayer outer surface. (11)

The corneocytes are joined together by modified desmosomes and overlap with each other at their edges to form a mechanically strong layer. (12)

The turnover time of the stratum corneum, the time for a newly formed cell to move from inside to outside and be sloughed, is approximately 14 days. (13)

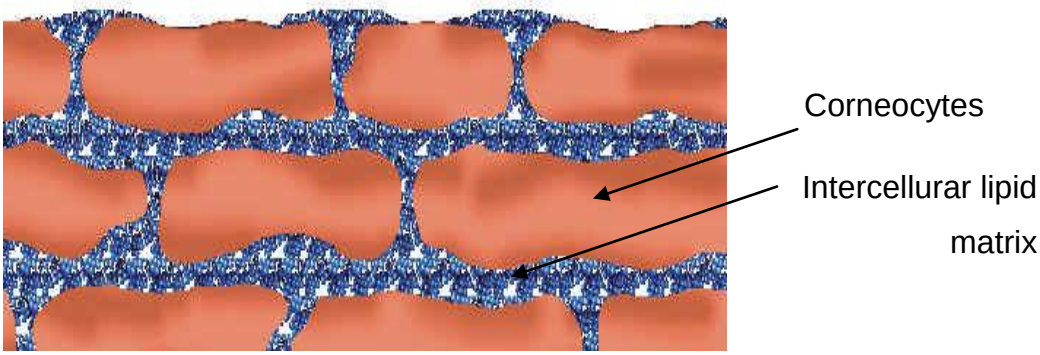

Figure 4: Brick and mortar model

2.1.1.1. Cutaneous metabolism

The viable epidermis is the most metabolically active layer in skin and is capable of chemically modifying a variety of molecules. The metabolic processes catalyzed by the enzymes present in the skin include oxidation, reduction, hydrolysis, and conjugation.

2.1.2.The dermis

The dermis (or corium) is 3 to 5 mm thick and is composed of a matrix of connective tissue in which predominant bundles of collagen fibrils interlace with elastic tissue (approximately 4%) and sparse reticular fibers (approximately 0,4%). This composite is embedded in an amorphous mucopolysaccharide ground substance comprising approximately 20% of the dermal mass. (7)

The dermis encloses cutaneous appendages (ecrine sweat glands, apocrine glands, and pilosebacious units) and is penetrated by blood vessels, lymphatics, and nerves. The cutaneous blood supply has an essential function in regulation of body temperature. It delivers oxygen and nutrients to the skin while removing toxins and waste products; the vasculature is vital in repairing damaged skin. Capillaries reach to within 0.2 mm of the skin surface and provide sink conditions for most molecules penetrating the skin barrier (other than extremely lipophilic molecules). The blood supply thus keeps the dermal concentration difference across the epidermis provides the essential driving force for transdermal permeation. (14)

2.1.3.The hypodermis

This is a fatty tissue representing the deepest part of the skin. It plays an important role in thermoregulation, insulation, provision of energy (nutritional store) and protection from mechanical injuries.

The main cells of the hypodermis are the adipocytes. Adipocytes are arranged in primary and secondary lobules.These lobules are separated by connective tissue septa containing cells (fibroblasts, dendrocytes, mastocytes), the

deepest part of sweat glands, as well as vessels and nerves contributing to the formation of the corresponding dermal plexuses.

2.1.4.Skin appendages

Hair follicles and their associated sebaceous glands (pilosebaceous glands), eccrine glands, apocrine glands, and nail plates are referred to as the skin's appendages. (7)

Hair follicles are found within the skin everywhere except the soles, the palms, the red portion of the lips and the external genitalia. Collectively, hair follicles occupy about 1/1000 of the skin's surface (15), a factor that sets a limit on the role they can play as a route of permeation. Each hair follicle possesses one or more flasklike sebaceous glands. (16) The normal function of sebaceous glands is to produce and secrete sebum, a group of complex oils including triglycerides and fatty acid breakdown products, wax esters, squalene, cholesterol esters, and cholesterol. Sebum lubricates the skin to protect against friction and makes it more impervious to moisture.

Eccrine or salty sweat glands are found over the entire body, except the genitalia. They are particularly concentrated in the palms and soles. (17) Ecrine sweat is dilute (hypotonic), slightly acidic (pH ≈ 5.0 owing to traces of lactic acid) aqueous solution of salt. (7) Eccrine sweat glands are the main sweat glands in humans, playing a vital role in the process of thermoregulation. Its secretion is stimulated when the body becomes overheated through warm temperatures or exercice. Evaporation of the water of the sweat cools the body's surface and, therby, the body. Since the gland is innervated by autonomic nervous system, ecrine sweating is also stimulated emotionally.

Apocrine glands have highly regionalize locations and are found only in the axillae, in anogenital regions, and around nipples. Bacterial decomposition of apocrine secretion is responsible for human body smell. (7)

2.2. PERMEATION PATHWAYS THROUGH THE STRATUM CORNEUM

There are two general options for drug substances to permeate the stratum corneum: the transepidermal route and the transappendicular route. (18)

The transepidermal route can be divided into the transcellular and the intercellular route. Using the transcellular route, the drug has to cross the skin by directly passing through both the lipid structures of the stratum corneum and the cytoplasm of the dead keratinocytes. This is the shortest route for the drug substance, but presents significant resistance to permeation because they have to cross both lipophilic and hydrophilic structures. The more common route for drugs to permeate the skin is the intercellular route. (19) In this case the permeant overcomes the stratum corneum by passing between the corneocytes, that implies a lipophilic pathway. The skin appendages (glands and hair follicles) occupy only 0.1% of the total human skin surface but the penetration thorugh it may also be an important pathway for the penetration of topically administered substances (20) as ions and polar compounds. (21)

The percutaneous absorption is a spontaneous, passive diffusional process that takes the path of least resistance. Therefore, depending on the drug and the condition of the skin, either or both routes can be important. (22)

2.3. THE PERCUTANEOUS ABSORPTION

The absorption of substances from outside the skin to positions beneath the skin, including entrance into the blood stream, is referred to as percutaneous absorption.

2.3.1.The process of percutaneous absorption

The process of the percutaneous absorption (Figure 5) can be described as follows. When a drug system is applied topically, the drug diffuses passively out of its vehicle and, depending on where the molecules are placed they partition into either the stratum corneum or the sebum-filled ducts of the pilosebaceous glands. Inward diffusive movement continues from these locations to the viable epidermis and dermis. In this way, a concentration gradient is established across the skin up to the outer ends of the skin’s microcirculation, where the

drug is swept away by the capillary flow and rapidly distributed throughout the body.

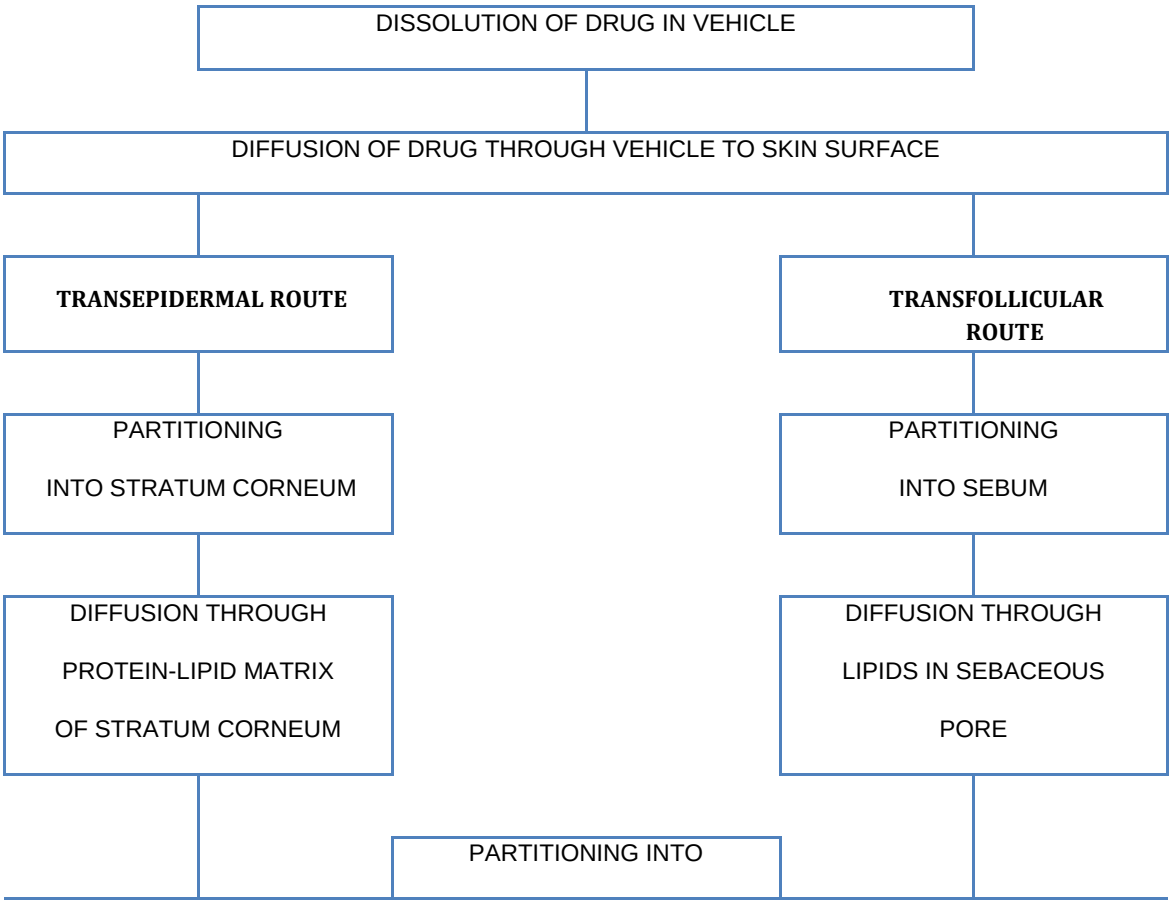

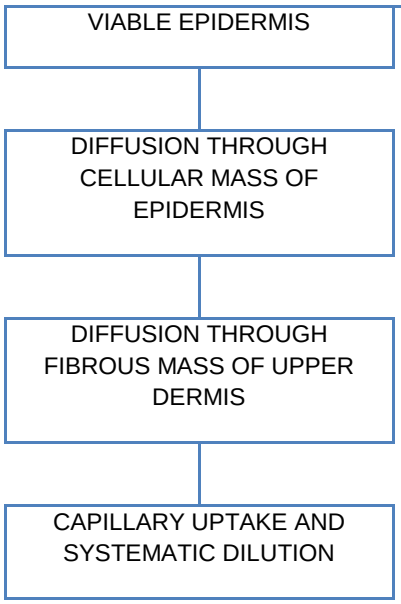

Figure 5: The process of the percutaneous absorption

2.3.2.Kinetics of absorption

Transport across the skin is by passive diffusion only . This is a phenomenon by which a diffusant moves down a concentration gradient by random molecular motion. In the situation of a permeant entering the skin, diffusion is usually considered as unidirectional. This unidirectional diffusion in an isotropic medium can be expressed mathematically by Eq. (1), Fick's second law of difusion,

$$\frac{\delta C}{\delta t} = D\frac{\delta^2 C}{\delta x^2}$$

Eq. (1)

where C is the concentration of the diffusing substance, x the space coordinate measured normal to the section, D the diffusion coefficient, and t the time. With skin permeation studies in vitro is often used a membrane clamped between two compartments, one containing a drug formulation (the donor) and the other a receptor solution providing sink conditions (essentially zero concentration), is often used. The pemeability coefficient of a diffusant through a membrane, K_p, may be defined following the Scheuplein diffusion model as described below. This author demonstrated (23) by Eq. (2).

$$Q_{(t)} = A \cdot P \cdot L \cdot C \cdot \left[D \cdot \frac{t}{L^2} - \frac{1}{6} - \frac{2}{\pi^2} \cdot \sum_{n=1}^{\infty} \frac{(-1)^n}{n^2} \cdot \mathrm{Exp}\left(\frac{-D \cdot n^2 \cdot \pi^2 \cdot t}{L^2} \right) \right]$$

Eq. (2)

The symbols used stand for: $Q_{(t)}$ (mg) is the quantity which passes through the membrane and reaches the receptor solution at a given time, *t* (min); *A* represents the actual diffusion surface area (cm^2); *P* represents the partition coefficient of the permeant between the membrane and the donor vehicle; *L* , the membrane thickness (cm); *D* is the diffusion coefficient of the permeant in the membrane (cm^2/h); and *C* is the concentration of the permeant (mg/ml).

After sufficient time, steady state diffusion across the membrane prevails. Under these conditions Eq. (1) may be simplified to Eq. (3).

$$\frac{dQ}{dt} = \frac{DC_0}{h}$$

Eq. (3)

where Q is the cumulative mass of permeant that passes per unit area through the membrane in time t; C_0 is the concentration of diffusant in the first layer of the membrane at the skin surface contacting the source of the penetrant; and h is the membrane thickness.

In most diffusion experiments, it is difficult to measure C_0, but C_0', the concentration of diffusant in the donor phase bathing the membrane, may be determined, because C_0 and C_0' are related, as shown by Eq. (4).

$$C_0 = PC_0'$$

Eq. (4)

where P is the partition coefficient of the diffusant between the membrane and the bathing solution. Substitution of Eq. (4) into Eq. (3) yields Eq. (5).

$$\frac{dQ}{dt} = \frac{DC_0'P}{h}$$

Eq. (5)

A graph of Q, the cumulative of drug crossing a unit area of skin, against time yields a profile of the drug penetrating the membrane.

Extrapolation of the pseudo-steady-state portion of the graph to the intercept on the time axis provides the lag time (L). This is the period during which the rate of diffusion across the membrane is increasing. Steady-state conditions prevail after approximately 2.7 times the lag time. (24) The lag-time is related to the diffusion coefficient by Eq. (6).

$$L = \frac{h^2}{6D}$$

Eq. (6)

Thus in theory, D may be obtained by measuring L, provided the membrane thickness, h, is known. In practice, this method for evaluating D has several disadvantages as the exact thickness of the stratum corneum is difficult to measure and may vary with penetration enhancer treatment. The measured thickness of the membrane does not allow for a tortuous pathway for diffusion and, for stratum corneum, the value obtained for D is therefore an apparent one.

The pemeability coefficient of a diffusant through am membrane, K_p, may be defined by Eq. (7).

$$K_p = \frac{PD}{h}$$

Eq. (7)

which may be substituted into Eq. (4) to give Eq. (8).

$$\frac{dQ}{dt} = C_0' K_p$$

Eq.(8)

The expression dQ/dt, the rate of change of cumulative mass of diffusant that passes per unit area through the membrane, is termed the flux of diffusant, J, and may be evaluated from the steady-state portion of a drug permeation profile. Hence, Eq. (9) holds.

$$J = C_0' K_p$$

Eq. (9)

2.3.3.Factors affecting percutaneous absorption

- Permeant properties

Some authors have agreed about the optimum conditions to be a good candidate to percutaneous administration. They can be summarized as follows:

- Low molecular weight (<600 Da), when its diffusion coefficient tends to be high
- Adequate solubility in oil water-so that the membrane concentration gradient (the driving force for difussion) can be high. Saturated solutions (or suspensions having the same maximum thermodynamic activity) promote the maximum flux
- A high, but balanced (optimal), partition coefficient (too large a value of K could inhibit the clearance by viable tissues)
- Low melting point, correlating with good ideal solubility (25)

- Variability of the skin

A matter of considerable consequence in topical delivery is variability in skin pemeability between patients. Differ in age, gender, race and health, all of which are alleged to influence barrier function.

The senile skin, which tends to be dry, irritable, and poorly vascularized, is actually barrier compromised. (26) Gender, too, affects the appearance of human skin. Nevertheless, there is little evidence that the skins of male and female differ much in permeability. There are established differences in the barrier properties if skin across the races of man. Although the horny layers of whites and blacks are of equal thickness, the latter has more cell layers and is measurably denser. As a consequence, black skin tends to be less permeable. (27)

Humidity and temperature also affect permeability. The skin hydratation increases skin permeability. The thermal activation alone can double the rate of skin permeability when there is 10º change in the surface temperature of the skin. (28)

The health of the skin establishes its physical and physiological condition, and, thus, its permeability. Broken skin represents a high-permeability state, and polar solutes are several log orders more permeable when administered over abrasion and cuts. Irritation and mild trauma tend to increase the skin's permeability, even when the skin is not broken.

2.4. MODULATION OF SKIN PERMEATION

The success of transdermal drug delivery systems depends on the ability of the drug to permeate skin in sufficient quantities to achieve therapeutic plasma levels. Unfortunately, many drugs do not posses, intrinsically, any great ability to cross the skin, and ways must be find to modify the barrier. This can be achieved chemically by the use of penetration enhancers or physically by the use of techniques such as iontophoresis or sonophoresis.

- ✓ Chemical enhancement

Substances reported to render the SC more permeable include alcohols, polyalcohols, pyrrolidones, amines, amides, fatty acids, sulphoxides, esters, terpenes, alkanes, surfactants and phospholipids. (29)

There are different mechanism of action of these enhancers because of their structural diversity. For example, alcohols solubilize and extract the lipid

component of the SC to facilitate permeation. (30) Fatty acids are able to induce lipid fluidization as well as phase separation within the membrane. (31) By contrast simple hydration does not appear to affect lipid bilayer conformation or spacing. (32) 1-dodecylazacycloheptan-2-one (Azone®) is effective at low concentration and is thought to act by lipid fluidization as well as ionpairing. (33)

- ✓ Physical penetration enhancement

The iontophoresis technique applies a small electric current (usually <500 μA cm^{-2}) to facilitate the transfer of drugs across the skin. (34)
Phonophoresis or sonophoresis uses ultrasound energy for the skin penetration enhancement of drug

2.5. TRANSDERMAL DRUG DELIVERY SYSTEM

Transdermal drug delivery systems are designed to facilitate the passage of drug substances from the surface of the skin, through its various layers, and into the systemic circulation.

Patch-type transdermal delivery systems are based on three design principles:

- Drug in adhesive
- Drug in matrix
- Drug in reservoir

In the last, the reservoir is separated from the skin by a rate-controlling membrane.

Although there are many differences in the design of transdermal drug delivery systems, several features are common to all systems including

- the release liner
- the pressure-sensitive adhesive
- the backing layer

all of which must be mutually compatible for a successful product. (35)

The adhesives are usually based on silicones, acrylates, or polyisobutylene. (36) The adhesive must be soft enough to ensure initial adhesion, yet have sufficient cohesive strength to be removed cleanly, leaving no residue.

A variety of materials can be used to fabricate the backing material and release liner. These include polyvinyl chloride, polyethylene, polypropylene, ethylene vinyl acetate and aluminium foil. The main property of these materials is that they should be impervious to the drug and other formulation excipients. (37)

Several materials can be used as rate-controlling membranes, examples being ethylene vinyl acetate copolymers, silicones, high-density polyethylene, polyester elastomers, and polyakrylonitrile. The membrane should be permeable only to the drug and the enhancer (if present) and should retain other formulation excipients. (38) In the matrix type is the drug uniformly dispersed in a polymeric matrix through which diffuses to the surface of the skin. (39) The polymeric matrix may be comprised of silicone elastomers, polyurethanes, polyvinyl alcohol, polyvinylpyrrolidones,etc.

The drug reservoir is usually made from simple formulations such as mineral oil, to complex formulations such as aqueous alcoholic gels. A definite requirement for a reservoir system is that it should be capable of permitting zero-order release of the drug over the delivery period. This requires the reservoir material to be saturated with the drug over the period of product application, which can be achieved by formulation the drug as a suspension.

Among the advantages of transdermal drug delivery systems are the following:

- ✓ They are easy to apply, can remain on place for up to 7 days (depending on the system), and are easily removed following or during therapy.
- ✓ The reduced dosing frequency and the production of controllable and sustained plasma levels tend to minimize the risk of undesirable side effects sometimes observed after oral delivery. (40) They avoid hepatic first-pass metabolism. Although the viable epidermis contains enzyme systems capable of metabolizing many drugs. (41)

A major disadvantage of transdermal drug delivery system is the potential for localized irritant and allergic cutaneous reaction. (42)

Modern TDS consist on self-adhesive matrices. Hydroxypropyl methyl cellulose is an atoxic polymer which provides transparent films with good organoleptic properties. It is also compatible with many cosolvents and enhancers used for

transdermal delivery. Besides that, the desired adhesiveness can be achieved by changing its concentration in the matrix. (5)

2.5.1. Drug release from HPMC-based pharmaceutical systems

The overall drug release mechanism from HPMC-based pharmaceutical devices depends on the design of the particular delivery system. The following phenomena are involved: at the beginning of the process, step water concentration gradients are formed at the polymer water interface resulting in water imbibition into the matrix. (43) Due to the imbibition of water swells resulting in dramatic changes of polymer and drug concentrations, and increasing dimensions of the system. Upon contact with water the drug dissolves and (due to the concentration gradients) diffuses out of the device. With increasing water content the diffusion coefficient of the drug increases substantially. (44)

2.6. MOLECULE UNDER THE STUDY

2.6.1. Pharmacological and pharmacokinetics of NTH

Nortriptyline hydrochloride is a tricyclic antidepressant widely used in the treatment of unipolar depression. Besides that, there is growing evidence of its efficacy for smoking cessation pharmacological therapy. (45) In both indications, its mechanism of action consists of the inhibition of noradrenalin reuptake and, to a lesser extent, of 5-HT. Chronic administration induces beta-receptor down-regulation. It presents a lower activity on alfa-adrenergic, histaminic and antimuscarinic than tertiary amines.

Nortriptyline is well absorbed, a plasma peak occur 2±3 h after oral administartion and half-life is about 24±48h. Its metabolism is primarily by hepatic oxidation to 10-hydroxy-nortriptyline, which may contribute to therapeutic and toxic effects. This metabolite is excreted intact by the kidneys.

The most common side effects are dry mouth, sweating, constipation, asthenia, tachycardia, headache, somnolence and dizziness. (46)

2.6.2.Physical-chemical properties

Nortriptyline hydrochloride structure is represented in Figure 6. It has a molecular weight of 299.8.

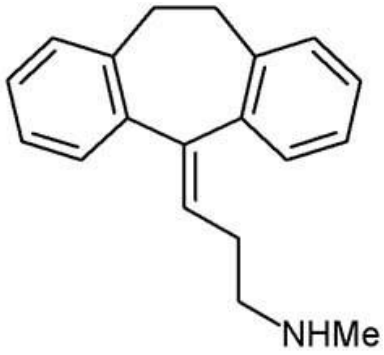

Figure 6: Nortriptyline hydrochloride

It exhibits a pKa value of 9.73, due to the presence of the amino tertiary group.

It is very soluble in water. The solubility in phosphate buffer has been experimentally found to be dependent on the pH. The reported values are 27.80±1.74 mg/ml at pH 5.5 and 0.72 ± 0.002 mg/ml at pH 7.4. It is soluble in alcohol and practically insoluble in ether. Its solubility in propylene glycol is 366.8±1.90 mg/ml. (1)

The lipophilicity of the tested substance measured as n-octanol partition coefficient pH of 5.5 for is 48.56±0.98. It has also been determined the partition coefficient beween HSE (heat separated epidermis) and the phosphate buffer pH 5.5 as 12.8±1.8. (1)

3. EXPERIMENTAL PART

3.1. FILM PREPARATION

A patch containing NTH was designed in a preliminary study. (1) It served as basis for the preparation of four different films with increasing concentration.

3.1.1.The composition of assayed films

The composition of films is shown in Table 1. The procedure to obtain a clear and uniform film is described underneath.

COMPOUND	PERCENTAGE (w/w)
NTH	5; 7.5; 10 or 15
Ethanol	30
Propylen glycol	30
Oleic acid	1
Polysorbate 80	1
(Hydroxypropyl)methyl cellulose	2
Distilled water adjusted to pH 5,5	c.s.

Table 1: Composition of assayed films

3.1.2.Procedure of preparation

A mixture of propylen glycol, ethanol and distilled water was prepared and NTH was dissolved in it under the stirring, with a speed of 500 rpm. The the solution was stirred for 5 minutes. Polysorbate 80 and oleic acid were incorporated and the mixture was stirred overnight.

HPMC was weighted and slowly incorporated to the prepared vehicle increasing the stirring speed to 800 rpm. It was allowed to hydrate for 24 hours. The amount of polymer remained constant because it is well known that the change on the polymer content in the film can modify the diffusive mobility of the drug in the polymeric network. (47)

Once it was fully hydrated and gel consistence was obtained, about 5 g of each preparation, exactly weighted, was placed into a Petri-dish, respectively about 15 g, exactly weighted, was placed onto plate of glass (BIO-R) (Figure 7). Gel was dried for 4 hours into an oven. The preparation was weighted again after this drying and stored in vegetal paper, to evade the exposition of ambient.

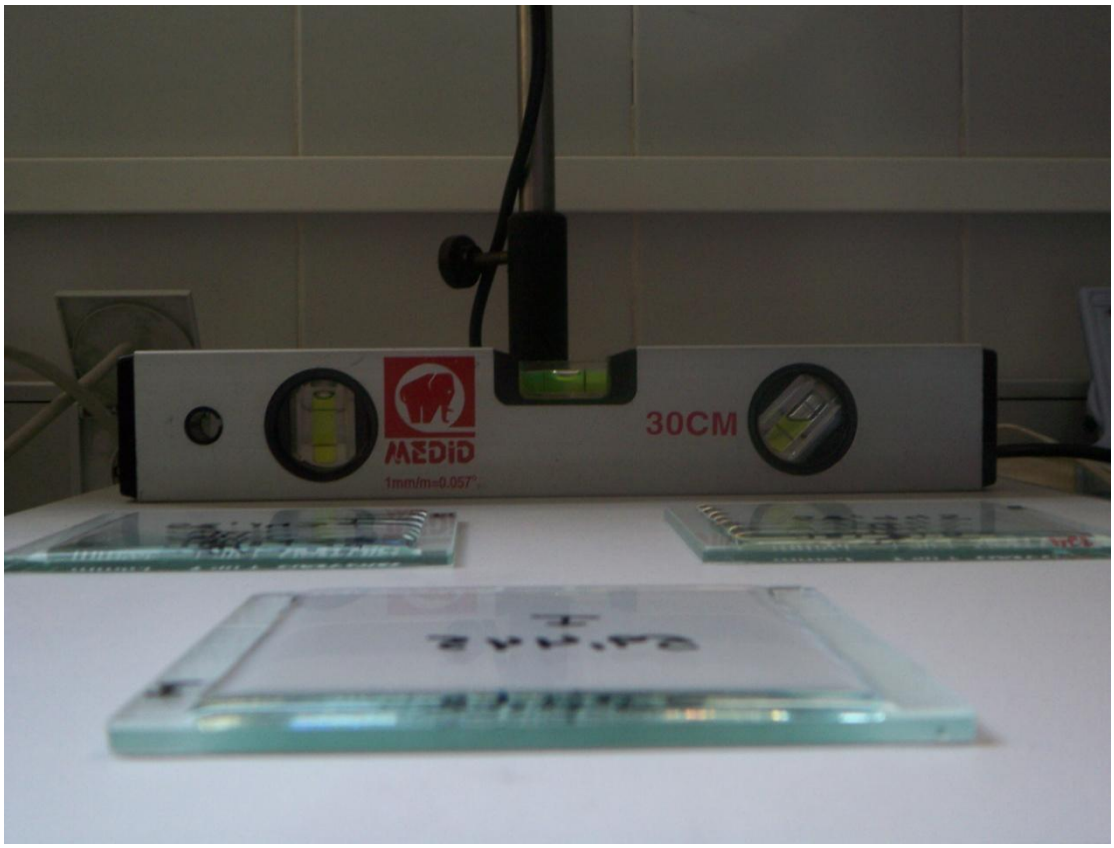

Figure 7: NTH film preparation

3.2. FILM CHARACTERIZATION

3.2.1. Film thickness

The thickness of the films was measured at three different points (micrometer control super EWX 0-25mm Ezquerra Micra). Mean values were calculated and are reported.

3.2.2. Film transparency

The film once dried was visually controlled for transparency by means of superposition over the clear foundation with black printed letters. This is considered as a quality index.

3.3. NTH IN VITRO DIFFUSION EXPERIMENTS

Two types of diffusion experiments were performed: release studies and in vitro permeation studies.

Both experiences were carried out using glass Franz type diffusion cells (FDC). Figure 8 schematically represents the setting. Two different FDC models were

used: one with an available diffusion area of 0.78 cm^2 and 6 ml of receptor cell volume and another with an available diffusion area of 1.327 cm^2 and 9ml of receptor volume. FDC were placed in heating/stirring module set at 35^0C to mimic the temperature of the skin surface.

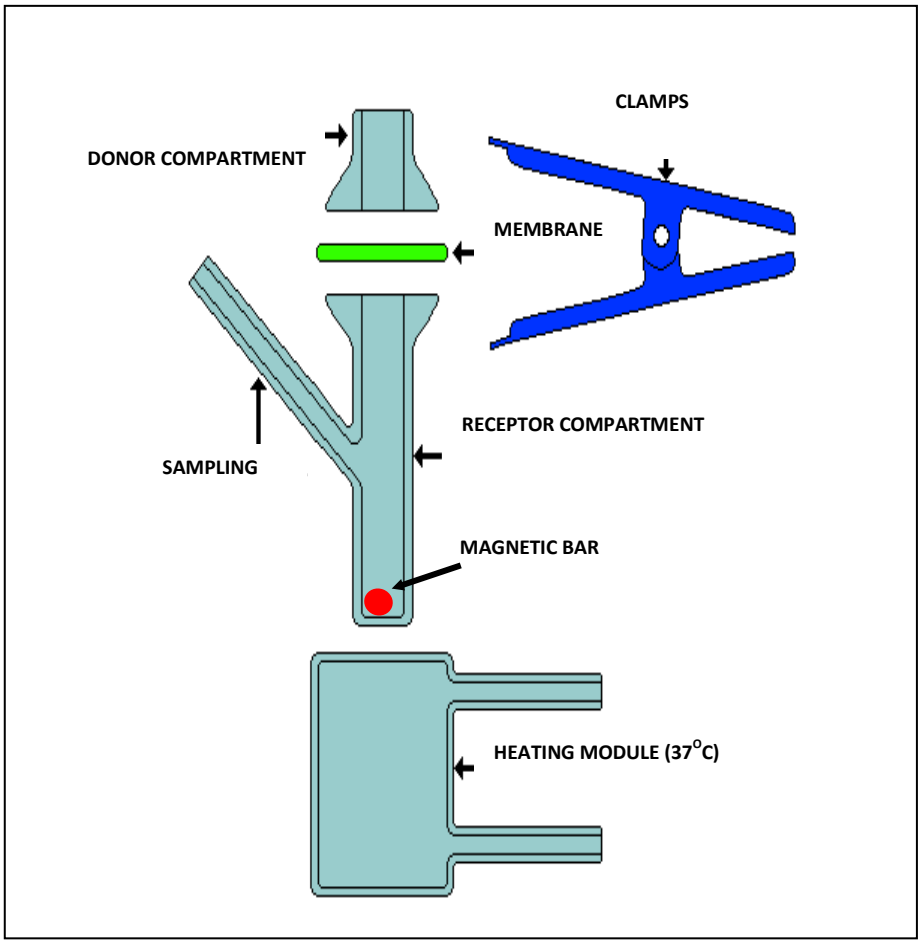

Figure 8: Diffusion cell, Franz type
http://www.scfonline.com/english/37_e/images37_e/Skinpenetration37_11_small.jpg

3.3.1.Buffer preparation

The receptor compartment was filled with phosphate buffer 1/15 M. The buffer is prepared as mixture 96:4 (V/V) of solution A and B. The buffer was adjusted to pH 5.5.

- Solution A

  It was prepared by dissolving 9.073g of NaH_2PO_4 in 1000 ml of water HPLC grade.

- Solution B

  This solution was prepared by dissolving 11.87g of Na_2HPO_4 in 1000 ml of water HPLC grade.

3.3.2.In vitro drug release study

The release of drug from film preparation was examined using FDC described above. The receptor compartment was filled with phosphate buffer 1/15 pH 5.5 solution free of air bubbles. A 25 mm circle of membrane (Millipore® nitrocelulose 0.45µm) was sandwiched between donor and receptor compartment. Prepared FDC were stabilized by clamps, placed in water bath (Figure 10) maintained at 35^0C and continually stirred by a magnetic bar at 500 rpm. After 10 min, cells were dosed by pressing sample patches onto the membrane. Parafilm or caps occluded the donor and receptor chambers respectively to prevent evaporation of volatile components. (48) Samples of 200 µL were withdrawn at specified intervals from the receptor compartment. The same volume of fresh buffer was replaced in the receptor after sampling.

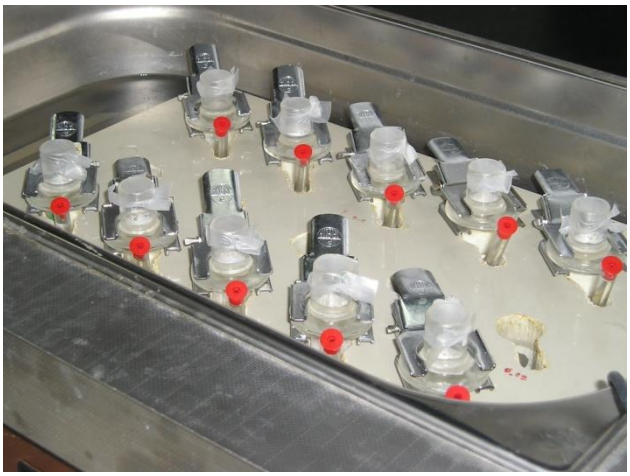

Figure 10: FDC in the heating/stirring module

3.3.3.In vitro skin penetration study

The penetration profile of NTH from film preparation was examined using FDC described above. The experimental conditions were the same as in vitro drug release study except for the type of membrane, that was heat-separated epidermis (HSE) obtained as described below. The skin pieces were mounted over the diffusion cells with the stratum corneum side in contact with the donor compartment and the dermal side over a dialysis membrane circle situated on the receptor compartment. The sampling was carried out every 90 min for a total of 72 h.

3.3.3.1. Skin sample preparation

Experiments were performed on abdominal skin samples from female donors aged 38 to 48 years, obtained after cosmetic surgical corrections performed in the Hospital 9 de Octubre (Valencia, Spain). Informed consent was previously obtained from the patients. Their identity was masked to the researchers to guarantee their anonymity.

Immediately after surgery, the skin was transported to the laboratory, where the excess fatty and connective tissues were carefully excised. The skin was cut into pieces with sufficient size for experiments. Damaged areas, with stretch or other marks, were left out because the experiments must be carried out with completely uniform samples. These pieces were wrapped in aluminium foil and stored in a freezer bags in freezer at -40º C for less than three months.

When required, the skin was removed from the freezer and left at room temperature (25^{o}C) to defrost for 1 to 2 hours. Epidermal membranes were prepared by a heat-separation technique. (49) The piece of skin was extended on a silicon plate and then it was fixed with needles. The plate with skin was sunk in distilled water kept at 60 ºC, for 45 s. This temperature debilitates the epidermis and dermis junction.

After 45s , the skin was took out of the bath and put into Petri dish containing 0.9% isotonic solution of NaCl (30 s approximately) to cool and to remove the rest of debris. Immediately after the epidermis was carefully separated from the underlying dermis (Figure 9). Circular discs of diameter 25mm were cut out and gently located on a filter paper (Whatman n^{0}1).

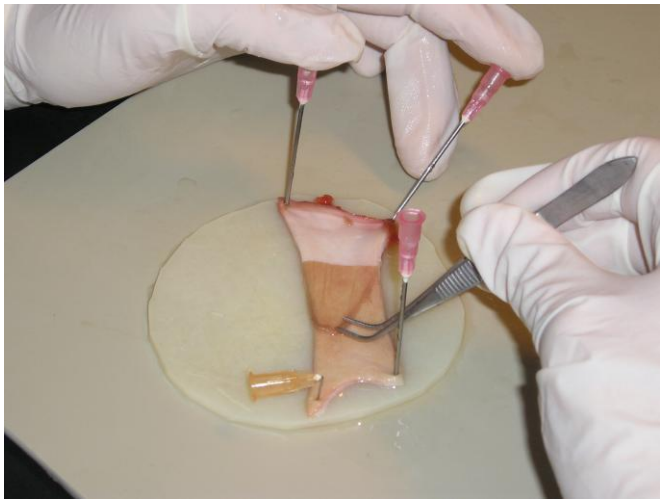

Figure 9: Separation of epidermis

3.3.3.2. Test of membrane integrity

Integrity of the epidermis was tested at the end of in vitro penetration experiments by means of the phenol red test. It consists of adding 400 µl of 1% phenol red solution into the donor compartment. The receptor compartment changed the color (Figure 10) if the membrane was damaged. The entire set of samples obtained from this cell was discarded in this case.

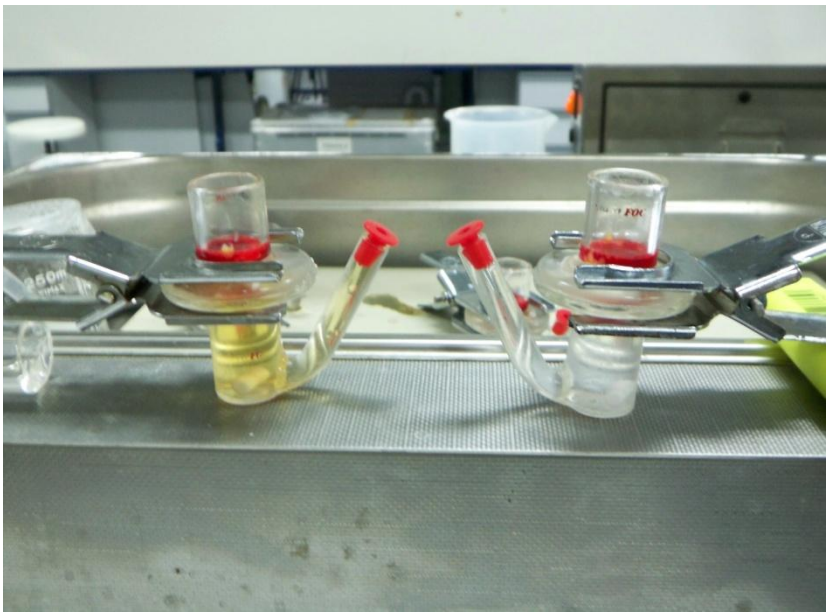

Figure 10: Phenol red test

3.4. ANALYTICAL METHOD FOR NTH DETERMINATION

NTH analysis was performed by high performance liquid chromatography.

3.4.1.HPLC equipment

The chromatographic system consisted of a isocratic bomb Waters model 1515, automated sample injector Perkin-Elmer series 200, UV detector Waters model 2487 and software Breeze 3.2® (Waters Co).

3.4.2.The mobile and stationary phase

The mobile phase was a mixture of acetonitrile HPLC grade (Scharlau) and phosphoric acid solution at 50/50 V/V.

The phosphoric acid solution was prepared by dissolving 1.17 g of NaH_2PO_4 in distilled water HPLC grade. The solution was adjusted to pH 3.

A Kromasil®RP-18 (150x4 mm, 5 µm) column a stationary phase was used as stationary phase.

3.4.3.Condition of analysis

The injection volume was 25 µl of each sample. The flow rate was 1. 0 ml/min. The wavelength of 254 nm was employed. Analysis was realized at ambient temperature. In these conditions, the retention time of NTH was about 2.3 min.

3.4.4.Method validation

The HPLC method was validated for linearity, accuracy and precision.

The linearity was checked by the determination coefficient of the linear regression of areas versus concentration, which represents the percentage of the response variability that can be explained by concentration. The significance of the regression is also demonstrated by F test that is provided by Excel®.

Accuracy was measured by the relative error calculated on three standards (low, medium and high concentration). Four replicates of every standard were injected onto HPLC on different days of analysis. It is reported as the maximum value and should be lower that 10 % and independent on the concentration.

Precision is established by the coefficient of variation of a set of four replicates, analysed on different days. Three levels of concentration were used (low, medium and high). In order to guarantee the quality of results it must be below 10%.

The limit of determination was also determined to ensure the appropriateness of the method for our experimental conditions. It was calculated as 3.3 times the standard deviation of the intercept divided by the slope of regression line.

3.5. MATHEMATICAL METHODS

The results are expressed as media and standard deviation, calculated by means of Excel 7.0. The variability is also reported as variation coefficient when appropriate. Linear regression was used for calibration curves. It was performed by means of Excel 7.0. The goodness of the fits was evaluated by the coefficient of determination (r^2) and the signification of the slope.

Nonlinear regression analysis was used to estimate the parameters of drug release and drug penetration across HSE. Sigmaplot 10.0 was used as software. No weighting scheme was used.

Akaika criterion was used to compare the goodness of the fit of the different kinetic models of release.

3.6. Determination of release parameters

Concerning drug release, the cumulative amounts of NTH versus time were plotted and its kinetics was characterized by fitting the Power law equation (Eq.10) and First order equation (Eq.11) to data. (44)

$$\frac{Qt}{Qinf} = k \cdot tn$$

Eq. 10

$$Qt = Q_{inf}\left(1 - e^{k.t}\right)$$

Eq. 11

In these equations, Q_t and Q_{inf} stand for the absolute cumulative amount of drug released at time *t* and infinite time, respectively, *k* represents a constant incorporating structural and geometric characteristics of the matrix, and *n* is the release exponent, indicative of the mechanism of drug release.

3.7. Determination of permeation parameters

In the case of permeabilty characterization, the cumulative amount of drug permeated through the skin was plotted as a function of the time. The permeability coefficients, K_p and lag time, t_L, were calculated following the Scheuplein diffusion model (Eq.12) .

$$Q_{(t)} = A \cdot P \cdot L \cdot C \cdot \left[D \cdot \frac{t}{L^2} - \frac{1}{6} - \frac{2}{\pi^2} \cdot \sum_{n=1}^{\infty} \frac{(-1)^n}{n^2} \cdot \mathrm{Exp}\left(\frac{-D \cdot n^2 \cdot \pi^2 \cdot t}{L^2} \right) \right]$$

Eq. 12

The symbols used stand for: $Q_{(t)}$ (mg) is the quantity which passes through the membrane and reaches the receptor solution at a given time, *t* (min); *A* represents the actual diffusion surface area (cm^2); *P* represents the partition coefficient of the permeant between the membrane and the donor vehicle; *L* , the membrane thickness (cm); *D* is the diffusion coefficient of the permeant in the membrane (cm^2/h); and *C* is the concentration of the permeant (mg/ml). In order to estimate K_p and t_L as primary parameters, equation 1 was transformed by substituing *P D/L* by K_p and $L^2/6D$ by t_L. The fitting equation (Eq.13) was:

$$Q_{(t)} = A \cdot Kp \cdot C \cdot \left[t - t_L - \frac{12 \cdot t_L}{\pi^2} \cdot \sum_{n=1}^{\infty} \frac{(-1)^n}{n^2} \cdot Exp\left(\frac{-\cdot n^2 \cdot \pi^2 \cdot t}{6 \cdot t_L} \right) \right]$$

Eq. 13

The symbols have already been described.

The flux was calculated using the following expresion (Eq.14):

$$J = Kp \cdot \Delta C \cdot A$$

Eq. 14

In which *J* stands for flux, *ΔC* represents the concentration gradient during the experiment and *A* is the diffusion area. Considering that conditions were representative of infinite dose experiments, it is assumed that, the concentration in the donor doesn't change more than 10% and therefore, it can be considered to be constant; the receptor phase is considered to be a sink, so that, *ΔC*, can be substituted by the concentration of the donor compartment.

4. RESULTS AND DISCUSSION

Patches of four different NTH concentrations were prepared and assayed for the release and penetration behavior. The results are described below along with the interpretation data. The patch of 5 %, 7.5 % 10 % and 15 %. The patch of 15 % has precipitated, consequently wasn't submitted to experiments. The appropriate patches were characterized by measuring its thickness. Film

transparency was also controlled. In vitro drug release and in vitro skin penetration study were performed using FDC.

4.1. VALIDATION OF THE ANALYTICAL METHODOLOGY

The HPLC method was validated for accuracy (9.6 as the highest relative error obtained), precision (2.7% as the highest variation coefficient) and linearity over the concentration range analyzed (r^2>0.999). The limit of determination was 50ng/ml.

4.2. FILM CHARACTERIZATION

The procedure for the preparation of the patch of 5%, 7.5%, 10% and 15% was similar. Nevertheless, during the desiccation process the 15% NTH patch precipitated, and consequently wasn't subjected to further experiments.

Patches with adequate organoleptic characteristics had their thickness measured at three different points of each patch. Three replicates were evaluated. The different measurements are listed in Table 2, along with the mean and standard deviation calculated.

Thickness [µm]				
Patch concentration	Measurement number			Mean±SD
	1	2	3	
5%	25	27	31	31.88±5.0
	30	35	38	
	27	36	38	
7,5%	30	29	26	32.33±5.1
	35	33	43	
	29	36	30	
10%	34	30	35	32.00±3.8
	30	27	27	
	32	35	38	

Table 2:Thickness of the patch [µm]. SD: standard deviation

As can be observed, this parameter remains constant regardless of the NTH concentration of the gel used to prepare the film. The variability is lower than 20 % in every case.

The amount of drug loaded in every type of patch was calculated and expressed as the ratio per area. The results are shown in Table 3.

Q total [mg/cm2]				
Patch concentration	Patch number			Mean±SD
	1	2	3	
5%	16.010	13.432	13.861	14.434±1.38
7.5%	18.810	21.505	22.293	20.869±1.83
10%	30.188	29.619	29.006	29.604±0.59

Table 3: Amount of NTH present in the different patches. SD: standard deviation.

Film transparency was also controlled. It was checked visually and confirmed for every patch prepared. By means of physical experiments, transparency observation and thickness measurement, it can be concluded that the films are homogenous.

4.3. CHARACTERIZATION OF THE RELEASE PROCESS

Drug release from the pharmaceutical dosage forms is a determinant parameter in *in vivo* performance, so that it should be studied in the design and development process of transdermal systems.

The experiences of release were performed with the three different patches assayed. The cumulative amounts released [mg/cm^2] from them are showed in Tables 4 to 6. Every table presents the raw data of the four replicates and the average and the standard deviation at each time point. The results are graphically outlined in Figures.

5%patch					
t(min)	Cumulative amount released Q [mg/cm2]				Mean cumulative amount±SD
	1	2	3	4	
10	1.161	0.760	0.778	0.584	0.821±0.24
20	3.099	1.415	1.394	1.520	1.857±0.83
30	3.426	2.284	1.880	2.173	2.441±0.68
40	3.916	2.909	2.407	2.894	3.032±0.63
60	4.595	3.595	2.691	3.548	3.607±0.78
120	6.168	5.555	3.804	4.820	5.087±1.02
180	6.672	6.374	4.636	5.626	5.827±0.91
265	8.805	7.282	5.337	7.129	7.138±1.42
360	-	7.128	5.911	7.552	6.864±0.85
420	-	7.342	5.887	7.865	7.031±1.02

Table 4: Cumulative amount of NTH released from 5% HPMC patch at the sampling times; mean, SD:standard deviation

7.5%patch					
t(min)	Cumulative amount released Q [mg/cm2]				Mean cumulative amount±SD
	1	2	3	4	
10	2.099	0.400	0.849	1.017	1.091±0.72
20	3.357	1.588	2.021	2.248	2.304±0.75
30	4.616	2.148	3.333	3.675	3.443±1.02
40	4.836	3.000	4.487	4.841	4.291±0.88
60	5.806	3.891	5.418	5.102	5.054±0.83
120	7.703	6.363	6.621	6.544	6.808±0.61
180	9.102	8.665	6.933	6.732	7.858±1.20
265	11.280	11.036	7.257	7.690	9.316±2.14
360	-	11.764	7.092	7.542	9.180±2.58
420	-	12.350	7.622	8.707	9.560±2.48

Table 5: Cumulative amount of NTH released from 7.5% HPMC patch at the sampling time; mean, SD: standard deviation

10%patch					
t(min)	Cumulative amount released Q [mg/cm2]				Mean cumulative amount±SD
	1	2	3	4	
10	1.414	3.476	1.020	1.12	1.757±1.16
20	6.160	5.659	2.309	2.81	4.234±1.96
30	9.047	7.467	3.591	4.62	6.180±2.52
40	10.516	8.442	5.129	6.10	7.546±2.42
60	12.461	10.070	6.772	7.87	9.293±2.52
120	16.207	13.344	11.137	13.23	13.479±2.08
180	18.836	15.900	13.982	0.68	12.349±8.03
265	20.363	21.412	16.858	32.35	22.745±6.69
360	-	-	17.620	19.98	18.802±1.67
420	-	-	17.860	19.22	18.538±0.96

Table 6: Cumulative amount of NTH released from 10% HPMC patch at the sampling time; mean, SD: standard deviation

The maximum cumulative amount released at 7 hours (last sampling point) varies as a function of the NTH concentration in the patch. It is always lower than the estimated content: 47%, 52% and 33% for 5%, 7.5% and 10% patch respectively). There is not a clear relationship between percentage released and patch concentration. The explication of this result could be a possible retention of NTH by the matrix of HPMC.

Two different kinetic models were fitted to the obtained data in order to get an insight into the mechanism underlying the process of release. They correspond to the first order kinetics and the power law, as described in the Experimental part section. The parameters estimated are presented in Table 7 to 9, along with the figures representing the goodness of the fit. The results are graphically presented in the Figures no 11 to 13, as a blue or red line (first order or power law fitting, respectively).

5% patch release kinetics				
First order	**Qinf±S.E. [mg/cm2]**	**k±S.E. [h-1]**	**r2**	**AIC**
	7.849±0.60	0.017±0.00	0.922	-33.251
	7.381±0.09	0.012±0.00	0.998	-69.309
	5.777±0.20	0.011±0.00	0.979	-53.468
	7.732±0.29	0.009±0.00	0.982	-48.995
Naive averaging data: Qinf=6.968±0.18[mg/cm^2]; k=0.013±0.00[h^{-1}]; r^2>0.986				
Standard two stage method: Qinf: 7.185±0.30[mg/cm^2]; k= 0.012±0.00[h^{-1}]				
Power law	**Kd±S.E.**	**n±S.E.**	**r2**	**AIC**
	0.045±0.01	0.445±004	0.967	-40.228
	0.043±0.01	0.439±0.05	0.936	-36.585
	0.032±0.00	0.442±0.03	0.981	-54.840
	0.033±0.01	0.484±0.03	0.977	-46.536
Naive averaging data: Kd=0.043±0.01; n=0.413±0.04; r>0.952				
Standard two steps method: Kd: 0.038±0.01; n: 0.453±0.04				

Table 7: Parameter describing release kinetics: Qinf-predicted amount released at infinite time; k first order release constant; r^{2-}determination coefficient; AIC-Akaike criterion, kd-diffusive constant; n-release exponent of the power law equation S.E.-standard error of the parameters.

7,5% patch release kinetics				
First order	**Qinf±S.E. [mg/cm2]**	**k±S.E. [h-1]**	**r2**	**AIC**
	20.675±1.97	0.003±0.00	0.907	-22.534
	13.736±0.35	0.006±0.00	0.998	-67.078
	7.307±0.17	0.020±0.00	0.984	-61.200
	7.719±0.29	0.019±0.00	0.956	-50.214
Naive averaging data: Qinf=9.135±0.34[mg/cm^2]; k=0.014±0.00[h^{-1}]; r^2>0.984				
Standard two steps method: Qinf: 12.359±0,69[mg/cm^2]; k=0.012±0.00[h^{-1}]				

Power law	Kd±S.E.	n±S.E.	r2	AIC
	0.054±0.00	0.424±0.01	0.997	-57.522
	0.015±0.00	0.617±0.05	0.980	-46.159
	0.054±0.02	0.325±0.06	0.848	-38.745
	0.052±0.01	0.343±0.05	0.906	-42.654
Naive averaging data: Kd=0.031±0.01; n=0.400±0.04; r>0.946				
Standard two steps method: Kd= 0.044±0.01; n=0.427±0.04				

Table 8: parameter describing release kinetics: Qinf-absolute cumulative amount released at infinite time; r^{2}-confidence interval; AIC-Akaike criterion, kd-diffusive constant; n-release exponent of the power law equation S.E.-coefficient standard error

10% patch release kinetics				
First order	Qinf±S.E. [mg/cm2]	k±S.E. [h-1]	r2	AIC
	36.468±4.13	0.004±0.00	0.862	-15.708
	41.523±3.08	0.003±0.00	0.951	-24.255
	18.968±0.27	0.007±0.00	0.999	-70.644
	20.374±0.39	0.009±0.00	0.997	-50.570
Naive averaging data: Qinf=18.721±0.65[mg/cm^2]; k=0.012±0.00[h^{-1}]; r^2>0.995				
Standard two steps method: Qinf=29.333±1.97[mg/cm^2]; k=0.006±0.00[h^{-1}]				
Power law	Kd±S.E.	n±S.E.	r2	AIC
	0.071±0.01	0.407±0.02	0.979	-34.306
	0.053±0.01	0.456±0.02	0.989	-38.864
	0.024±0.01	0.552±0.05	0.962	-38.687
	0.029±0.01	0.528±0.06	0.960	-30.596

Naive averaging data: Kd=0.045±0.02; n=0.455±0.08; r>0.844
Standard two steps method: Kd=0.044±0.01; n=0.486±0.04

Table 9**:** parameter describing release kinetics: Qinf-absolute cumulative amount released at infinite time; r^{2}-confidence interval; AIC-Akaike criteria, kd-diffusive constant; n-release exponent of the power law equation S.E.-coefficient standard error,

As can be observed there is not a general best model to describe the data. Both are useful in order to predict the maximum amount to be released and the rate at which the process will be developed. On the other hand, two different approaches have been used to describe the whole batch, i.e. naïve averaging data (NAD) and standard two steps (STS) fitting method. The NAD method was applied to data fitting the equation to the mean amount released at every sampling time, even though the variability between replicates was relatively high (maximum value of 22.9%, 24.2% and 33% for 5%, 7.5% and 10% patch, respectively). STS method has the advantage of establishing the inter-subject variability of parameter estimations, which are quite low in this case. Both method estimate very similar parameters characterizing the release process.

Considering the 5%patch from a statistical point of view (i.e. Akaike criterion), two replicates are slightly better described by the power law equation and the other two for first order kinetics. If first order results are taken into account, the maximum value to attain represents about 7 mg/cm^2, regardless of the fitting approach used. The release first order constant is estimated as 0.012 h^{-1}. This means that 57.7h would be needed to release the maximum amount. These data are in accordance with the low percentage of NTH released from the patch. Considering the power law equation, result obtained with 5% patch show that release mechanism is basically fickian diffusion as the exponent is between 0.45 and 0.5, which are representative of a cylinder and a film respectively. This fact explains good results obtained when applying the first order equation. Moreover, the fact can be explained considering that the patches obtained were not completely flat (31.88μm).

In consideration to the 7.5% patch from a statistical point of view (i.e. Akaike criterion) one replicate is slightly better described by the power law equation and the other three for first order kinetics. If first order results are taken into account, the maximum value to attain represents about 12mg/cm^2, in reference to STS method. The release first order constant is estimated as 0.012 h^{-1}. This means that 57.7h would be needed to release the maximum amount. As mentioned above, it is in accordance with the low percentage of NTH released from the patch. The release mechanism is basically fickian diffusion, the exponent is also above 0.4 to 0.6.

In reference to 10% patch, two replicates are slightly better described by the power law equation and the other two for first order kinetics, from a statistical point of view (Akaike criterion). If first order results are taken into account, the maximum value to attain in release represents about 29 mg/cm^2, in regard to STS method. The release first order constant is estimated as 0.06 h^{-1}, it means that 115.5 hours would be needed to release the maximum amount. It is in accordance with the low percentage released from the patch. The release mechanism is basically fickian diffusion, as the exponent is between 0.4 to 0.5.

NTH release; 5% patch

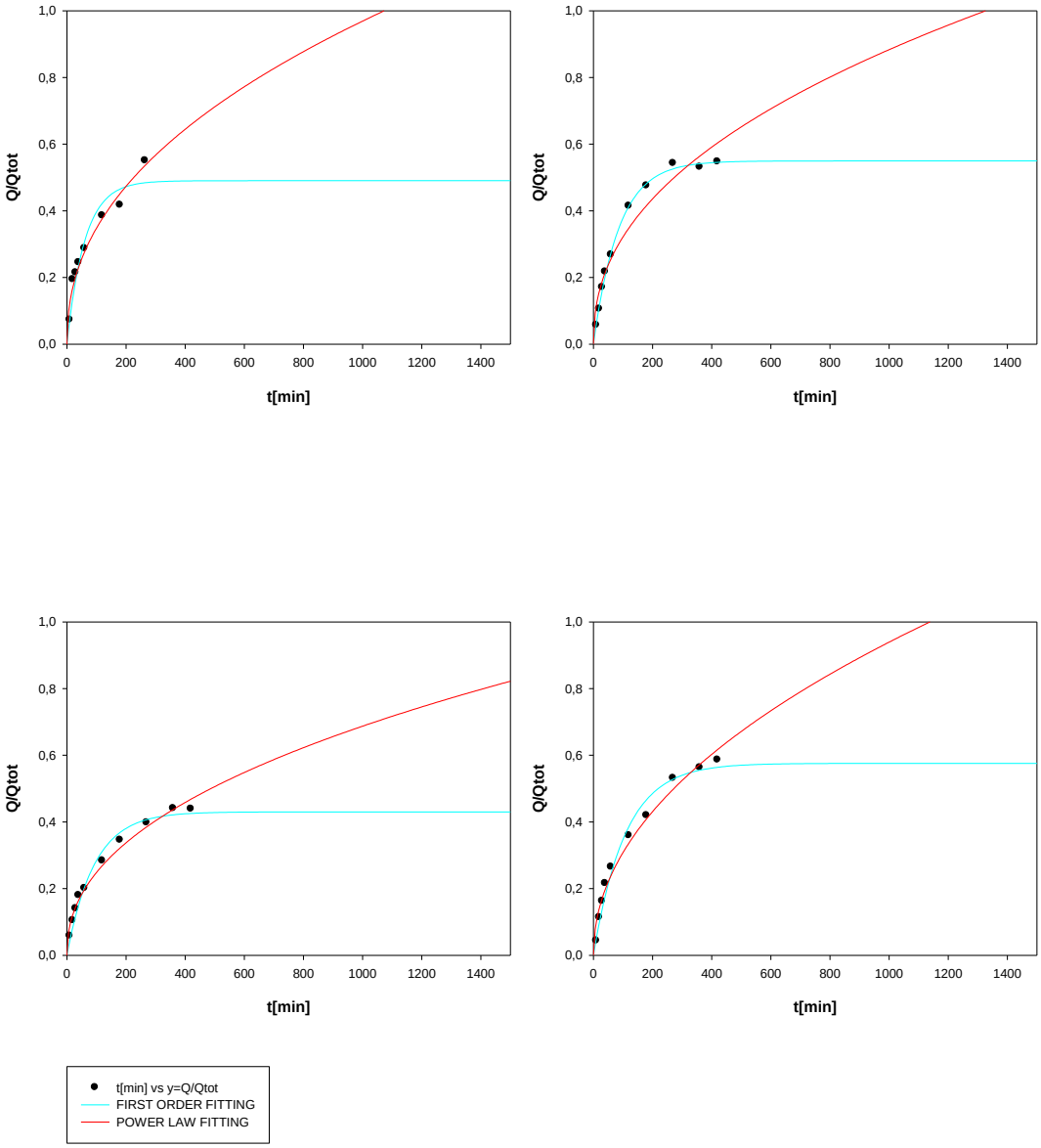

Figure 11: in vitro drug release of NTH from 5% patch in static Franz diffusion cells.

NTH release; 7.5% patch

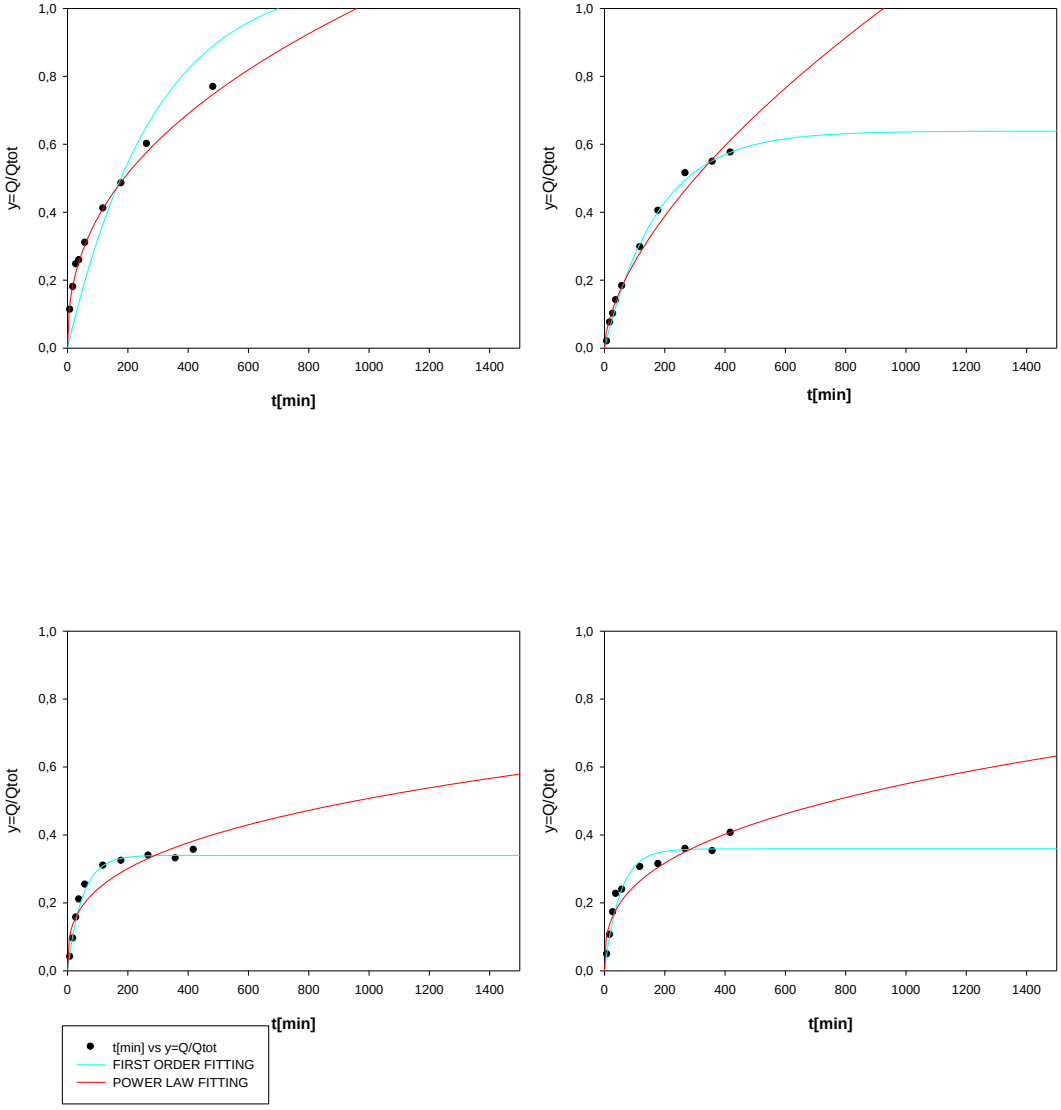

Figure 12: in vitro drug release of NTH from 7.5% patch in static Franz diffusion cells.

NTH release; 10% patch

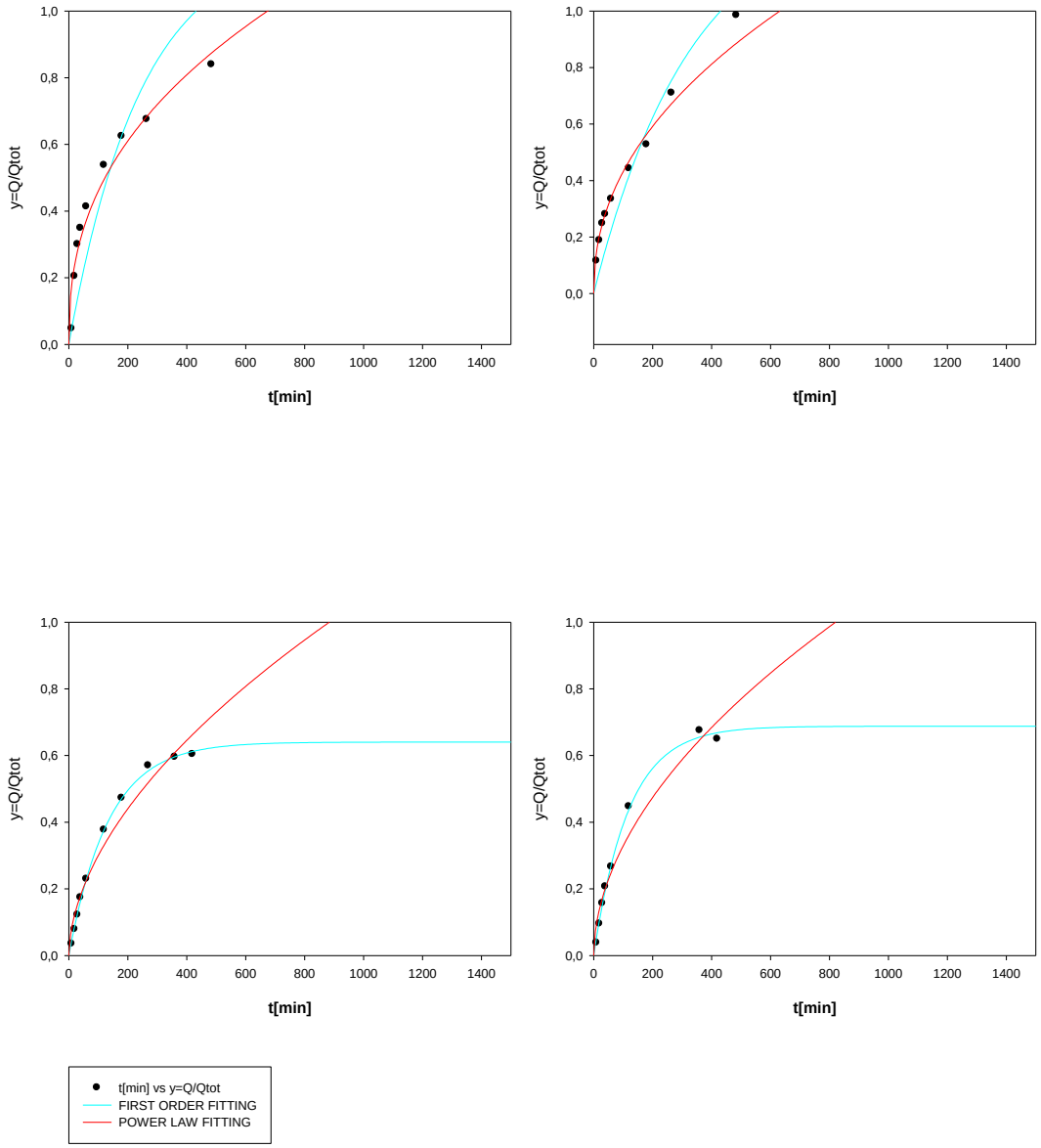

Figure 13: in vitro drug release of NTH from 10% patch in static Franz diffusion cells.

4.4. CHARACTERIZATION OF PENETRATION THROUGH HSE

The cumulative amount of NTH that penetrated through HSE discs was calculated for each sampling time as described in Experimental part section. The Scheuplein equation was fitted to the obtained data. Only the STS method was used as the sampling time was not homogeneous. The estimated parameters by this method are presented in Table 10, along with the figures representing the goodness of the fits. The figures 14 to 16 illustrate the relationship between amount of NTH permeated per area and time for different concentration patches.

5%patch		
Kp± S.E. [cm/h] ·10^{-3}	r2	t0±S.E. [h]
0,017± 0,00	0,999	56,835±1,94
0,022± 0,00	0,992	48,880±2,87
0,013± 0,00	0,999	47,188±1,35
0,022± 0,00	0,992	52,188±3,54
Standard two stage method: Kp=0.019·10^{-3}±0.00 [cm/h]; t0=51.273±2.42[h]		

Table 10: NTH penetration through the human skin parameters (K_p-permeability coefficient; r^2-coefficient of the linear regression of experimental versus predicted data points; t_0-lag time; S.E.-parameter standard error)

7.5%patch		
Kp± S.E.[mg/cm]	r2	t0±S.E.[h]
0,010·10^{-3}± 0,00	0,999	45,318±1,96
0,003·10^{-3}± 0,00	0,996	19,202±2,90

$0{,}002 \cdot 10^{-3} \pm 0{,}00$	0,968	33,667±2,24
$0{,}001 \cdot 10^{-3} \pm 0{,}00$	0,996	14,207±0,80
Standard two stage method: $Kp = 0.004 \cdot 10^{-3} \pm 0.00$ [mg/cm]; t0=28.099±1.97[h]		

Table 11: NTH penetration through the human skin parameters (K_p-permeability coefficient; r^2-coefficient of the linear regression of experimental versus predicted data points; t_0-lag time; S.E.-parameter standard error)

10%patch		
Kp± S.E.[mg/cm]	**r2**	**t0±S.E.[h]**
$0{,}005 \cdot 10^{-3} \pm 0{,}00$	0,998	46,127±2,52
$0{,}007 \cdot 10^{-3} \pm 0{,}00$	0,987	25,184±2,86
$0{,}003 \cdot 10^{-3} \pm 0{,}00$	0,998	10,280±1,42
$0{,}003 \cdot 10^{-3} \pm 0{,}00$	0,996	23,697±1,12
Standard two stage method: $Kp = 0.005 \cdot 10^{-3} \pm 0{,}00$[mg/cm]; t0=26.312±1.98[h]		

Table 12: NTH penetration through the human skin parameters (K_p-permeability coefficient; r^2-coefficient of the linear regression of experimental versus predicted data points; t_0-lag time; S.E.-parameter standard error)

The extended lag time (around 50h) indicates that the steady state is not achieved during the experimental period. It is a drawback of the formulation presented that should be addressed in future designs.

In order to increase the flux through the skin, the increase in patch concentration was assayed. The lag time is decreasing with increasing concentration. As the Kp of 5%patch is anomalously high, the previous studies on NTH patches reported coefficients around 0.003 $cm \cdot h^{-1}$, only flux of 7.5% and 10% patches were calculated. The result is $0.834 \cdot 10^{-6}$ [mg^2cm/g] for 7.5%

patch and $1.291 \cdot 10^{-6}$ [mg^2cm/g] for 10%patch. It can be concluded that the increasing drug concentration increases the drug flux.

.

5%patch

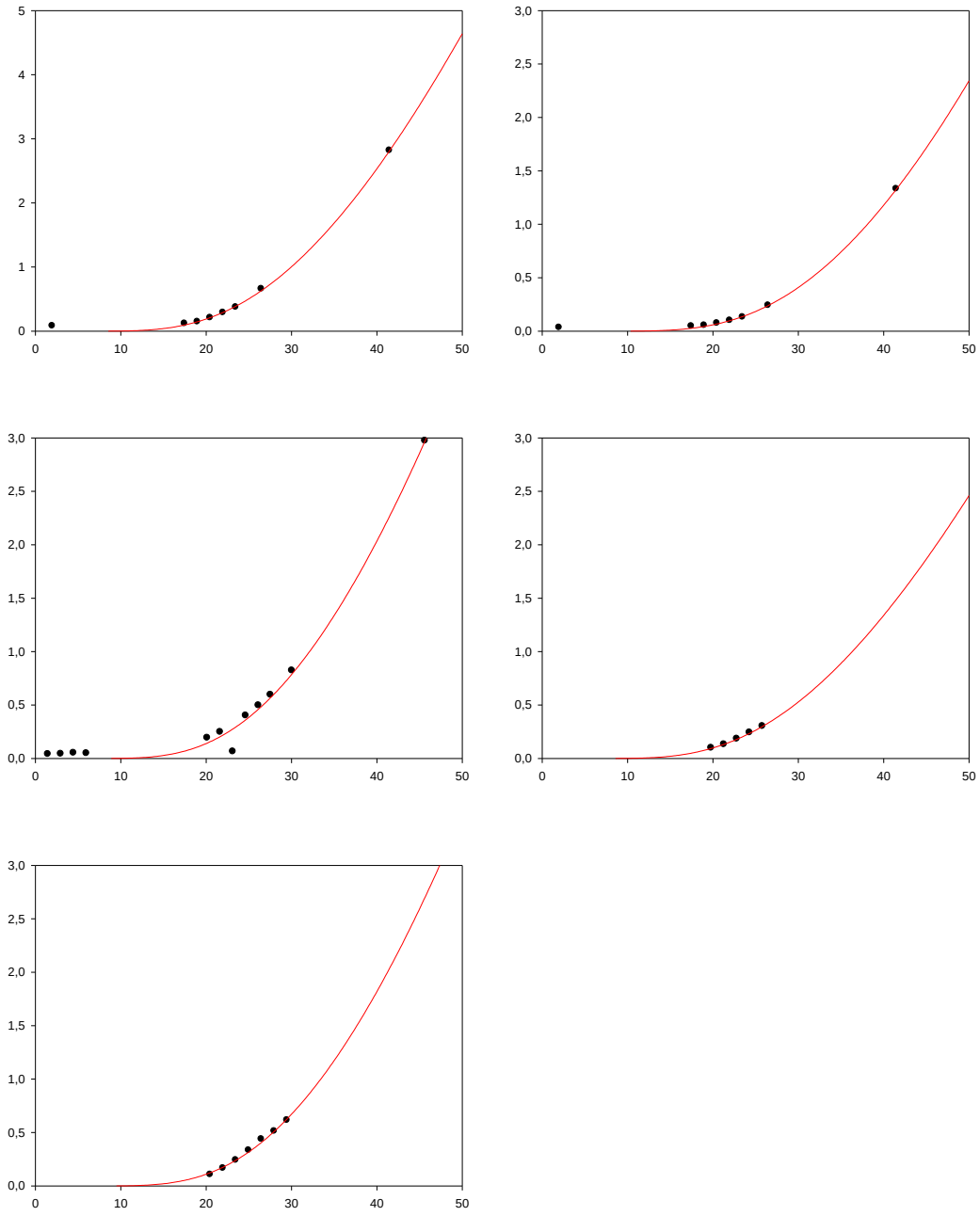

Figure 14: penetration profile of NTH through the human skin; 5%patch; x=Q[mg/cm^2]; y=t[h

7.5%patch

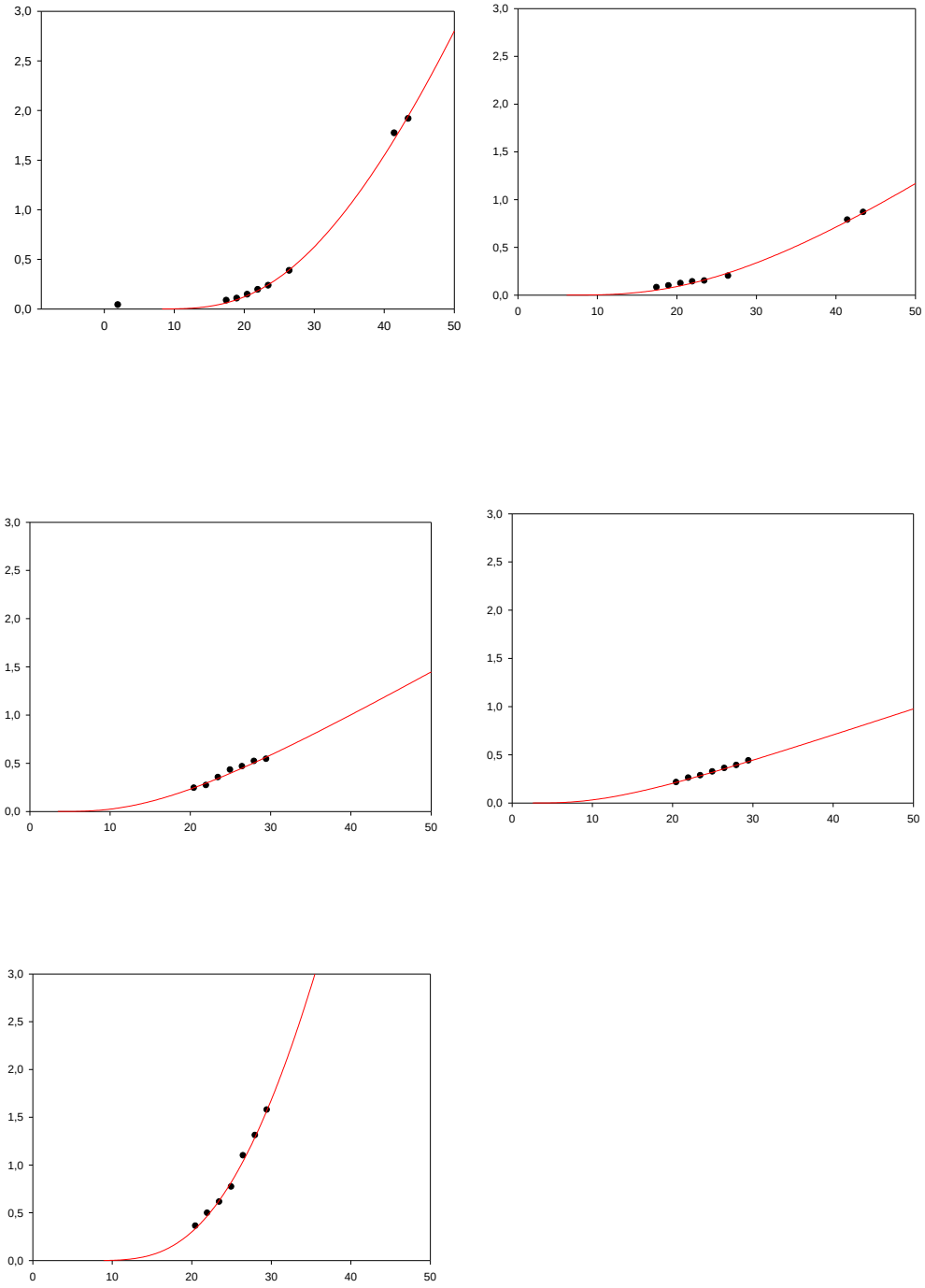

Figure 15: Penetration profile of NTH through the human skin; 7.5%patch; x=Q[mg/cm^2]; y=t[h]

10%patch

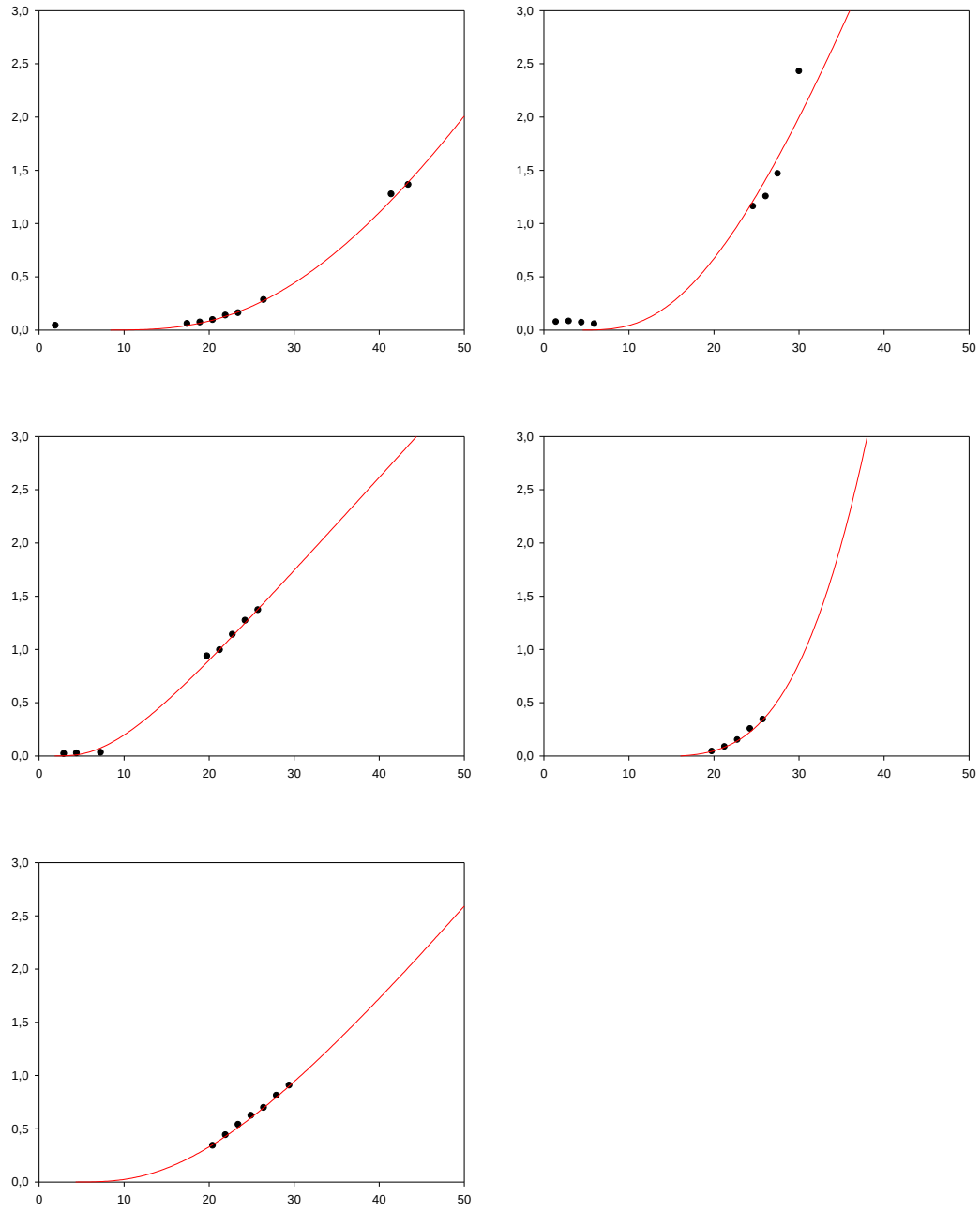

Figure 16: penetration profile of NTH through the human skin; 10%patch; x=Q[mg/cm^2]; y=t[h]

5. SUMMARY AND CONCLUSIONS

The object of this study was to investigate effect of NTH concentration incorporated in (hydroxypropyl)methyl cellulose patch on physical and biopharmaceutical properties of essayed films with a intended aim to develop controlled drug release system to help smokers to quit.

Using NTH, antidepressant drug, in the smoking cessation is secure, with a good tolerance a lower cost, if we compare it with others substances, like bupropion, recommended in the specialized bibliography as alternative for the first line treatment.

As described in the theoretical part, selection of the transdermal route is based on the appropriate physical-chemical properties of the drug and better patient's compliance for this type of administration than for oral route.

Between different possibilities of the transdermal delivery system, drug-in-matrix design principle was chosen. It's technologically easier to prepare small scale. Besides that it's more economic than the other designs, question relevant for pharmaceutical form with presumptive commercialization. Moreover, because of its thinness, it's more discrete for patients to apply.

Essential patch constituent, (hydroxypropyl)methyl cellulose (HPMC), was selected because it is an atoxic polymer which provides transparent films with good organoleptic properties. Its safety profile is well established through a large experience in its use. Furthermore, the desired adhesiveness can be achieved by changing its concentration in the matrix.

Patches of 5%, 7.5% and 10% NTH concentrations were studied for the physical, release and penetration characteristics.

According to the presented results it can be concluded that the thickness remains constant regardless of the NTH concentration of the gel used to prepare the film. The homogeneity of the films was macroscopically established.

The maximum cumulative amount released at the last sampling point varies as a function of the NTH concentration in the patch. Nevertheless there is not a

clear relationship between percentage released and patch concentration. This might be explained by retention of NTH by the matrix of HPMC.

From reported results, it seems evident that both assayed kinetic models, first order and power law, are useful in order to predict the amount released and the rate at which the process will be developed. The release mechanism is basically fickian diffusion.

Considering penetration experiments, the above-described results have shown that the lag time decreases with increasing patch concentration, so that only 7.5 and 10% NTH patch are promising. Taking into account that the provided flux depends directly on the concentration, the conclusion is that 10%patch is the design to be develop a TDS useful practice.

6. ABREVIATIONS

EtOH	Ethanol
FDC	Franz diffusion cells
HPMC	(Hydroxypropyl)methyl cellulose
HSE	Heat separated epidermis
NaCl	Sodium chloride
NAD	Naïve Averaging Data
NTH	Nortriptyline Hydrochloride
STS	Standard Two Steps method
TDS	Transdermal Drug delivery System
WHO	World Health Organization

7. REFERENCES

1.**Melero A, Garrigues TM, Almudever P, Villodre AM, Lehr CM, Schafer U.** Nortriptyline hydrochloride skin absorption. Development of a transdermal patch. *Eur J. Pharm Biopharm.69(2).p558.* 2008.

2. **http://www.who.int/features/factfiles/tobacco/en/index.html.**

3. **DE., Jorenby.** Smoking cessation strategies for the 21st century. *Circulation 104.p51.* 2001.

4. **Jorenby DE, Hays JT, Rigotti NA, Azoulay S, Watsky EJ, Williams KE, Billing CB, Gong J, Reeves KR.** Efficacy of varenicline vs placebo or sustained release bupropione for smoking cessation. *JAMA.296.p56.* 2006.

5. **Hughes JR, Stead LF, Lancaster T.** Antidepressants for smoking cessation. *Cochrane Database Syst Rev.24(1):CD000031.* 2007.

6. **Rushmer RF, Buettner KJ, Short JM, Oland GF.** The skin. *Science.154(757).p343.* 1966, pp. 343-348.

7. **Wilkes GL, Brown IA, Wildnaner RH.** The biomechanical properties of skin. *Crit.Rev.Bioeng.1(4)p453.* 1973.

8. **Holbrook KA, Odland GF.** Regional differences in the thickness (cell layers) of the human stratum corneum:an ultrastructural analysis. *J Invest Dermatol.62(4).p415.* 1974.

9. **Scheuplein RJ, Morgan L.** "Bound water" in keratin membranes measured by a microbalance technique. *Nature.214.p456.* 1967.

10. **Bouwstra JA, Dubbelaar FE, Gooris GS, Ponec M.** The lipid organisation in the skin barrier. *Acta Derm Venereol. Suppl.208. p23.* 2000.

11. **Wertz PW, Madison KC, Downing DT.** Covalently bound lipids of human stratum corneum. *J Invest Dermatol.92.p109.* 1989.

12. **Kligman AM, Christophers E.** Preparation of isolated sheets of human stratum corneum. *Arch Dermatol. 88.p702.* 1963.

13. **Rothenberg S, Crounse RG, Lee JL.** Glycine-C-14-incorporation into the proteins of normal stratum corneum and the abnormal stratum corneum of psoriasis. *J Invest Dermatol.37.p497.* 1961.

14. **R., Marks.** The stratum corneum barrier-the final frontier. *J Nutr.134(8Suppl).p2017.* 2004.

15. **RJ, Scheuplein.** Mechanism of percutaneous absorption II.Transient diffusion and the relative importance of various routes of skin penetration. *J Invest Dermatol.48(1).p79.* 1967.

16. **RT, Woodburne.** Essentials of Human Anatomy. *Med Bul.28p25.* 1965.

17. **W, Montagna.** An introduction to sebaceous glands. *J Invest Dermatol.62(3).p120.* 1974.

18. **BC, Lippold.** How to optimize drug penetation through the skin. *Pharm Acta Helv.67.p294.* 1992.

19. **J, Hadgraft.** Skin deep. *Eur J Pharm Biopharm.58.p291.* 2004.

20. **Landeman J, Otberg N, Richter H, Jacobi U, Schaefer H, Blume-Peytavi U, Sterry W.** Folicular penetration.An important pathway for topically applied substances. *Hautarzt.54.p321.* 2003.

21. **RT, Tregear.** The permeability of mammalian skin to ions. *J Invest Dermatol.46.p16.* 1966.

22. **Scheuplein RJ, Blank IH.** Permeability of the skin. *Physiol rev.51.p.702.* 1971.

23. **Diez-Sales O, Garrigues TM, Herraez JV, Belda R, Martin-Villodre A, Herraez M.** In vitro percutanous penetration of acyclovir from solvent systems and carbopol; 971-P hydrogels: influence of propylene glycol. *J Pharm Sci.94(5)p1039.* 2005.

24. **BW, Barry.** *Dermatological Formulations:Percutaneous Absorption.p67.* NY : Marcel and Dekker, Inc, 1983.

25. —. Is transdermal drug delivery research still important today? *DDT Vol6.19p961.* 2001.

26. **Feldman RJ, Maibach HI.** Absorption of some organic compounds through the skin in man. *J Invest Dermatol.54.p399.* 1970.

27. **KW, Weingand.** Glycerol-blanked triglyceride assays with laboratory animals. *Clin Chem.36.p.2011.* 1990.

28. **Chang SK, Riviere JE.** Percutaneous absorption of parathion in vitro in porcine skin:effect of dose, temperature, humidity and perfusatecomposition on absortive flux. *Fundam Appl Toxicol.17.p494.* 1991.

29. **Purdon CH, Azzi CG, Zhang J, Smith EW, Maibach HI.** Penetration enhancement of transdermal delivery. *Crit Rev Ther Drug Carrier Syst.21(2).p97.* 2004.

30. **T, Kai.** Mechanism of percutaneous penetration enhancement:effect of n-alkanols on the permeability barrier of hairless mouse skin. *J Control Release.12.p.103.* 1990.

31. **Ongpipattananakul B, Burnette RR, Potts RO.** Evidence that oleic acid exists in a separate phase within straum corneum lipids. *Pharm Res.8.p.350.* 1991.

32. **Mak VH, Potts RO, Guy RH.** Does hydration affect intercellular lipid organization on the stratum corneum? *Pharm Res.8.p.1064.* 1991.

33. **Hadgraft J, Walters KA, Wotton PK.** Facilitated transport of sodium salicylate across an artificial lipid membrane by Azone. *J Pharm Pharmacol.37(10).p.725.* 1985.

34. **RH, Guy.** Iontophoresis-recent developments. *J Pharm Pharmacol.50(4).p371.* 1998.

35. **Baker RW, Heller J.** Materials Selection for Transdermal Delivery Systems. *Transdermal Drug Del.p. 293.* 1989.

36. **MC, Musolf.** Pressure-Sensitive Adhesives: Science and Engineering. *Transdermal Controlled Systemic Medications.p 93.* 1987.

37. **NM, Marecki.** Design considerations in transdermal drug delivery systems. *Proc 10th Pharm Tech Conf.p.311.* 1987.

38. **Yuk SH, Lee SJ, Okano T, Berner B, Kim SW.** Ona-way membrane for transdermal drug delivery systems. Membrane preparation and characterization. *Int J Pharmaceut.77.p.231.* 1991.

39. **Gopferich A, Lee G.** Measurement of drug diffusivity in stratum corneum membranes and a polyacrylate matrix. *Int J Pharmaceut.71.p.245.* 1991.

40. **Noonan PK, Wester RC.** Cutaneous Metabolism of Xenobiotics. *Drug delivery.Inc.56.p.53.* 1989.

41. **Ahmed S, Imai T, Otagiri M.** Stereoselective hydrolysis and penetration of propranolol prodrugs: in vitro evaluation using hairless mouse skin. *J Pharm Sci.84.p.877.* 1995.

42. **RJ, Schmidt.** Cutaneous side effects in transdermal drug delivery: Avoidance strategies. *Transdermal drug delivery.53 p. 83.* 1989.

43. **Peppas NA, Lustig SR.** Solute diffusion in hydrophilic network structures. *Hydrogels in medicine and pharmacy.1.p.57.* 1986.

44. **Siepmann J, Peppas NA.** Modeling of drug release from delivery sustembased on hydroxypropyl methylcellulose. *Advenced drug delivery reviews.48.p.139.* 2001.

45. **JR, Hughes.** Mechanism of action of a decision aid for smoking cessation treatment. *Addiction.101. p.1362.* 2006.

46. **Lincova D, Farghali H.** *Zakladni a aplikovana farmakologie.p187.* s.l. : Galen, 2007.

47. **Padula C, Nicoli P, Colombo P, Santi P.** Single-layer transdermal film containing lidocaine:modulation of drug release. *Eur J Pharm Biofarm.66.p422.* 2007.

48. **Panchangula R, Salve PS, Thomas NS, Jain AK, Ramarao P.** Transdermal delivery of naloxone:effect of water, propylene glycol, ethanol and their binary combinations on permeation through rat skin. *Int J Pharm.219.p.95.* 2001.

49. **Kligman AM, Christophers E.** Preparation of Isolated Sheets of Human Stratum Corneum. *Arc Dermatol. 88.pp.702.* 1963.

8. ACKNOWLEDGEMENT

I would like to express my acknowledgement to Prof. Teresa M Garrigues for her patient, psychical support, advises and professional help with my work on this thesis.

I thank also Patricia A Folch for her assistance in laboratory.

I would like to thank doc.RNDr.Pavel Doležal, CSc, for his assistance by completing my thesis.

I thank also to Erasmus/Sokrates project for financial support and for great experience from Spain.

Last but not least I would like to thank my family for everything.